FINAL PUBLISHABLE JRP REPORT

JRP-Contract number	IND17
JRP short name	Scatterometry
JRP full title	Metrology of small structures for the manufacturing of electronic and optical devices
Version numbers of latest contracted Annex Ia and Annex Ib against which the assessment will be made	Annex Ia: V1.0 Annex Ib: V1.0
Period covered (dates)	From 1st October 2011 To 30th September 2014
JRP-Coordinator	
Name, title, organisation	Dr. Bernd Bodermann, Physikalisch-Technische Bundesanstalt
Tel:	+49 531 592 4222
Email:	bernd.bodermann@ptb.de
JRP website address	www.ptb.de/emrp/ind17.html
Other JRP-Partners	
Short name, country	CMI, Czech Republic DFM, Denmark MIKES, Finland NPL, United Kingdom VSL, The Netherlands Nanocomp, Finland

REG-Researcher 1 (associated Home Organisation)	Dr. Sven Burger JCMwave , Germany	Start date: 1st Dec 2011 Duration: 24 months
REG-Researcher 2 (associated Home Organisation)	Dr. Toni Saastamoinen UEF, Finland	Start date: 1st Nov 2011 Duration: 35 months
REG-Researcher 3 (associated Home Organisation)	Prof. Dr. Paul Urbach TU Delft, The Netherlands	Start date: 1st Oct 2012 Duration: 12 months
REG-Researcher 4 (associated Home Organisation)	Dr. Bernd Loechel HZB, Germany	Start date: 1st Nov 2012 Duration: 12 months

Report Status: PU Public

EMRP
European Metrology Research Programme
Programme of EURAMET

The EMRP is jointly funded by the EMRP participating countries within EURAMET and the European Union

TABLE OF CONTENTS

1 Executive Summary 3
2 Project context, rationale and objectives 4
3 Research results 6
3.1 Improvement of the accuracy, traceability and 3D capability of scatterometric methods 6
3.1.1 New and improved scatterometry methods 6
3.1.2 Limitations and approximations in scatterometry 8
3.1.3 Advanced data evaluation and statistical treatment 9
3.1.4 Modelling of realistic geometries 10
3.1.5 Measurement comparisons of 1D gratings 11
3.1.6 Modelling and data analysis of measurements of 2D gratings and 3D structures 13
3.1.7 Measurements on 2D gratings 14
3.2 Extension of scatterometric methods 17
3.2.1 Short wavelength scatterometry 17
3.2.2 Development of diffractive test structures on planar and curved substrates 18
3.2.3 Goniometric scatterometry for diffractive structures 19
3.2.4 Mueller polarimetry for diffractive structures 19
3.2.5 Characterisation and measurements on planar diffractive optical elements 20
3.2.6 Characterisation and measurements on curved diffractive optical elements 20
3.3 Development of ultra-high resolution microscopy (AFM, SEM) to support scatterometry and to enable measurements comparisons with scatterometry 21
3.3.1 X-ray coupled AFM 22
3.3.2 Long-range 3D AFM 23
3.3.3 Testing of structure details using AFM and SEM 25
3.4 Development of efficient and reliable methods for a combined data analysis of the different metrology methods 27
3.5 Design, development, test and calibration of a scatterometry standard 30
3.5.1 Design aspects 30
3.5.2 Process development and manufacturing 32
3.5.3 Sample characterisation 33
3.5.4 Calibration 37
4 Actual and potential impact 39
4.1 Dissemination 39
4.2 Impact on standardisation 39
4.3 Impact on the metrology and scientific communities 39
4.4 Impact on the industrial and other user communities 40
4.5 Long term impact 41
5 Website address and contact details 41
6 List of publications 42

1 Executive Summary

Introduction

This project developed sophisticated dimensional metrology of structures in the sub- micrometre range to support current and future manufacturing processes and further development of technologies for optics and semiconductor industries. Optical scatterometric methods and approaches have been developed and improved, supported by i) novel and sophisticated modelling and data analysis methods for scatterometry, and ii) improved and novel methods for atomic force microscopy (AFM). For the first time, traceable scatterometric measurements with a well-defined uncertainty budget and much improved agreement of measurement results between different scatterometer tools and other microscopic methods have been achieved. These achievements were supported by the development of the first scatterometry reference standard samples and a reliable calibration service for standard and customer samples.

The Problem

With the continuous shrinking of structure dimensions and a clear trend towards much more complex 3D structures for future nanoelectronic devices, it is crucial to develop improved measurement tools and methods appropriate to those dimensions. For future developments in the semiconductor industry, accurate and reliable measurements of the size of nanoelectronic device structures, the so called critical dimensions (CD), have been identified as essential but also as an unsolved problem. Currently, scatterometers and critical dimensions scanning electron microscope systems (CD-SEMs) are the main metrological tools used for production measurements. Scatterometry usually shows an excellent sensitivity to small changes in the dimensions of the structures. However, before this project, traceable and absolute scatterometric measurements were not available and product-related standards for the characterisation and calibration of scatterometers did not exist. As a consequence, scatterometric measurements often showed systematic deviations when compared with CD-SEM measurements. In the optics industry, diffractive optics and in particular the characterisation of curved structured surfaces, are becoming increasingly important. Currently, only microscopic measurement methods such as AFM or SEM, are used to test the size of diffractive structures. However, these microscopic methods are generally slow and not suited for manufacturing control of new optical devices.

The Solution

In response to these problems, the project set out to develop more accurate and traceable dimensional measurements of nanoelectronic structures, diffractive and hybrid optical components.

The project has developed:

- Improved or novel scatterometric methods and sophisticated modelling and data analysis methods to significantly reduce the measurement uncertainty to the 1 nm level;
- Traceable scatterometric measurements and suitable scatterometry reference standards;
- Improved dimensional metrology for diffractive structures based on scatterometric methods.

Impact

Direct uptake of the project's outputs, in particular low cost diffractive optics, provides European manufacturers such as Nanocomp access to fast and efficient optical metrology for manufacturing. This will enable improved and faster quality control and process development supporting the success and growth of manufacturers of diffractive optics. Different stakeholders such as manufacturers of scatterometry-based metrology tools and European manufacturers of integrated circuits have shown interest in the developed reference standard samples, and it is expected that several stakeholders will use these standard samples as soon as they are commercially available. The availability of reliable scatterometry reference standard samples and the knowledge and methods developed in this project will support manufacturers e.g. ASML, SENTECH in the development of their products and therefore contribute to support their already strong international European position. The improved and partly novel metrology capabilities developed within this project are already contributing to the development of new and better products of European semiconductor companies and in the longer term will contribute to sustain and extend the success of the European and international semiconductor industry. The project has also supported wider dissemination and uptake of its outputs via inputs to relevant standardisation bodies.

2 Project context, rationale and objectives

The *International Technology Roadmap for Semiconductor Manufacturing* (ITRS roadmap) has noted that the measurement capabilities of structure sizes are a critical component for future progress in technology and semiconductor industries. Different technology platforms and projects e.g. *European Technology Platform Nanoelectronics*, *Nanostrand (Standardization related to Research and Development for Nanotechnologies)* and *Co-Nanomet*, agreed that three-dimensional (3D) characterisation of small structures and speed of characterisation are global challenge topics for optical and semiconductor industries. Furthermore, as the size of features decrease, the significance of additional structure details on the intended structure function increases substantially.

The development of advanced lithography requires methods with exceptional measurement uncertainties for the metrology of 3D structures. For critical parameters such as the period of a grating structure or width of individual structures, uncertainty measurement values below one nanometre are necessary. This is emphasised by the term *critical dimension* (CD), which is used synonymously for the width of a structure. Metrology of these structure dimensions are one of the most challenging metrology tasks in this context.

In the semiconductor industry two types of methods are used for the characterisation and control of the critical structure dimensions: high resolution microscopic methods e.g. Atomic Force Microscopy (AFM) and Scanning Electron Microscopy (SEM), and optical methods based on the analysis of light scattered at the structured surfaces to be measured, so-called scatterometric methods. However, a systematic and coherent methodology to combine these different types of measurement tools has not been developed. Furthermore, there was not an accepted standard that could be used in these different measurement methods to match the results obtained from different instruments.

Even though scatterometry has some essential advantages over microscopic methods it was mainly used for in-line metrology. The ITRS roadmap noted that the combination of these methods would be the preferred solution for solving the continuing metrology demand for smaller structure sizes. However it also noted that there are challenges to be met before these methods can actually provide a practical solution. The combination of these different metrology techniques would require comparable and matching, i.e. traceable, results for both methods and the possibility to test and demonstrate this agreement, e. g. by using a reference standard sample suitable for all methods should be involved. An essential challenge was that scatterometric measurements were not traceable at the beginning of this project.

The scatterometry task force group of Semiconductor Equipment and Materials International (SEMI), which *serves the manufacturing supply chain for micro- and nano-electronics industries)* identified in 2010 the need for traceability and standardisation in scatterometry, which has also been demonstrated by the activities of the international association for Semiconductor Manufacturing Technology (SEMATECH) together with the US national standardisation institute NIST. At the beginning of this project there were neither suitable calibrated scatterometry reference standard samples nor an available calibration service for scatterometry test samples.

On the other hand, in the optics industry, the use of structured functional surfaces and diffractive optics is growing rapidly. Refractive-diffractive optics can replace multi-component products with a single component and thus produce miniaturised products. Diffractive and diffractive-refractive (so called hybrid) optical components are becoming more and more important in optics industry, but the characterisation of these components is also an enormous metrological challenge. Sub-nanometre precision measurements over a range of several millimetres have to be done in all dimensions, which before this project was only possible using specially developed 3D interferometer coupled Atomic Force Microscopes (AFMs). However, with scan rates of only a few ten µm/s those AFMs are not fast enough for in-line measurement of such large areas. The physical dimension of AFM tips also makes it impossible to measure narrow and deep structures, which must be taken into account in the design of reference samples. Furthermore, in the optics industry there was a lack of generally accepted standardised methods for the characterisation of diffractive optical microstructure. Scatterometry is a promising method to meet these challenges in optical industry, but there has to be tools and methods appropriate to meet the specific challenges of diffractive components such as the characterisation of diffractive structures on curved surfaces.

To overcome the limitations in optical scatterometry described above and to meet current and future metrology requirements this project addressed the following scientific and technical objectives:

1. *Improvement of the accuracy, traceability and 3D capability of scatterometric methods*
   - Improvement of the accuracy and traceability of scatterometric methods to the 1 nm range (for linewidth), corresponding to an improvement of one order of magnitude as compared with currently available linewidth metrology;
   - Improvement of the 3D capability, the efficiency and the measurement uncertainty, of scatterometric methods to achieve the suitability of scatterometry for applications in process development and quality control for 3D structures;
   - Evaluation of the sensitivity and robustness of scatterometric measurements to structure details;
   - Development of faster data analysis tools, which are 3D-capable and offer a reliable uncertainty estimation option and the flexibility to include complex structure geometries and detailed structure parameters
2. *Extension of scatterometric methods*
   - Methodical extension of scatterometry to shorter wavelengths (extreme ultraviolet - EUV, X-Ray), polarimetry and Fourier scatterometry;
   - Methodical extension of scatterometric methods for the characterisation of diffractive optical elements, especially on curved surfaces (diffractive-refractive optics);
3. *Development of ultra-high resolution microscopy (AFM, SEM) to support scatterometry and to enable measurements comparisons with scatterometry*
   - Development of ultra-high resolution microscopy (AFM, SEM) and short wavelength (EUV, GSAXS) scatterometry to deliver further structure details;
   - Combination of an AFM with x-ray and optical interferometry to provide high resolution measurements of local variations at the sub-nm level of grating periods;
   - Extension of the scatterometric and microscopic metrology systems used by this project partners to enable comparison measurements;
4. *Development of efficient and reliable methods for a combined data analysis of the different metrology methods*
   - Evaluation of the sensitivity of scatterometry to different structure details and implementation of *a priori* information delivered by additional (e. g. AFM-, SEM- or grazing incidence small angle X-ray scattering - GISAXS-) measurements in the data evaluation of scatterometry;
   - Development of efficient and reliable methods for a combined data analysis of different methods, both scatterometric and microscopic, with the aim to achieve measurement uncertainties well (i.e. more than 10%) below the individual measurement uncertainties;
5. *Design, development, test and calibration of a scatterometry standard*
   - Design, development, test and calibration of a scatterometry standard, which basically is also suitable for AFM and SEM testing.

3 Research results

3.1 Improvement of the accuracy, traceability and 3D capability of scatterometric methods

Introduction

To enable traceable scatterometric measurement with the required accuracy and the capability to measure 3D structures in semiconductor industry different steps have been necessary. A full and detailed understanding of the measurement process was required and any sources of possible systematic measurement deviations had to be identified, investigated and quantified. Additionally the sensitivity of scatterometry had to be significantly enhanced in particular for measurements of sub-wavelength gratings and 3D-structures to meet the tough uncertainty requirements required by the semiconductor industry. For this purpose we investigated different scatterometry methods: some state-of-the art approaches have been further improved and some novel methods have been developed and tested. Due to the distinct features of these different methods we were able to

- investigate the corresponding sensitivities and advantages of different methods for specific applications and measurands;
- identify and differentiate characteristic sources of systematic measurement errors for different methods.

The data analysis, i.e. the reconstruction of the dimensional structure parameters and structure geometry (including the determination of the optical parameters of the structure and substrate materials) are an essential part of scatterometric measurements and usually require a long time and computational power resources. Since these resources are always limited, in particular in industry applications, approximations and simplifying assumptions are typically applied, which limits the measurement uncertainties and the applicability of scatterometry and may lead to significant systematic measurement deviations. Fast, reliable and realistic modelling and data analysis ask for significant improvements in modelling speed, data evaluation, statistical treatment and reliable and improved uncertainty estimations. Thus, to substantially decrease the measurement uncertainties and increase the range of suitable applications of scatterometry we have worked on faster and advanced rigorous modelling methods, have implemented more realistic structure geometries, improved significantly the data analysis, statistical treatment and uncertainty estimation procedures and applied these improvements to the characterisation of two-dimensional structures.

The characterisation of the 3D geometry of nanostructures is very important for example for the characterisation of contacts or line end features in nanoelectronic manufacturing. However, real 3D metrology is still a challenge for scatterometry as well as for microscopic methods. For scatterometry the challenges result from the enormous requirements on computational resources on the hand, and on the requirement to measure and analyse also the conical diffraction, in contrast to 2D structures such lines of a 1D line grating, where in principle the analysis of the in-plane diffraction, the co-planar diffraction pattern, is sufficient (this is of course only true, if roughness is neglected, since roughness is always a 3D feature). Two different scatterometry approaches have been developed and tested for their 3D capability, Fourier scatterometry and GISAXS combined with an area detector.

Discussion

3.1.1 New and improved scatterometry methods

Within this project we have improved existing and developed new scatterometry methods.

DUV scatterometer and spectroscopic Ellipsometer

PTB has modified and improved its unique self-made DUV scatterometer to meet the requirements and enable the planned investigations within this project: The system, which was originally designed to measure photomasks, was equipped with a versatile wafer holder with vacuum chuck to mount the wafer based samples to be investigated. The signal-to-noise ratio of the detection has been improved by three orders of magnitude to provide the required parameter sensitivities. Finally, a means has been added to enable systematic variations of the illuminating spot size at the sample between 40 µm and and 4 mm to study possible spot size effects experimentally.

PTB has used additionally a commercial spectroscopic ellipsometer (DUV to NIR) to get *a priori* information (such as optical material parameters and layer thickness of the investigated samples) and to characterise the

geometry parameters of the nanostructures, the latter in comparison with, as well as in a hybrid approach using combined analysis with scatterometry data.

Mueller polarimetry

Polarimeters are optical instruments used for determining the polarisation properties of light beams and samples. Sample-measuring polarimeters determine the polarising action of a sample that can be measured analysing transmitted, reflected, diffracted or scattered light. Measurements are acquired using a series of polarisation elements located between source and sample, and the existing beams are analysed with a separate set of polarisation elements between the sample and detector. Mueller matrix algebra describes all the 16 different polarisation states combinations that can be measured in polarimetry. The polarisation properties contain a considerable amount of detailed information about the (structured) surface. However, up to now, only best classical ellipsometers are in use for the characterisation of such surfaces. The additional information provided by Mueller polarimetry is quantitatively and qualitatively a substantial extension of the information gathered with conventional scatterometry, giving Mueller Polarimetry a much higher surface sensitivity for grating structure parameters. This is in particular true for stochastic scattering at rough surfaces or line edged as well as for polarisation mixing structure geometries or orientations, such as line endings or 3D structures in general.

Within this project DFM's Mueller polarimeter has been used for extensive investigations of 1D gratings and curved multi-patterned diffractive structures (see fig. 11).

Accurate polarimetric measurements can be made only if the polarisation generator and the polarisation analyser are fully calibrated. To perform accurate polarimetry, the polarisation elements do not need to be ideal. If the Mueller matrices of the polarisation components are known, the systematic errors due to non-ideal polarisation elements can be removed during the data analysis. Considerable amount of work has been put into the metrological characterisation of all the hardware components of DFM's home built Mueller Polarimetry setup and the full metrological analysing software with uncertainty propagation. This work has been beyond state of art and of uttermost importance for removing the system errors and to reach the low measurements uncertainties demonstrated in this project.

Fourier scatterometry

With classical scatterometers or ellipsometers samples only the light emitted by the samples within the plane of incidence is analysed. While this works very well for 1D gratings/ 2D structures such as line gratings, for real 3D structures arranges in a 2D grating the conical diffraction has to be analysed as well. This can be achieved using Fourier scatterometry, a very fast and effective method. In a Fourier scatterometer the diffracted light is collected by a Fourier-lens and the exit pupil of this lens being the Fourier plane of the diffraction pattern is then imaged onto an image detector. DFM and PTB both have set-up and tested a Fourier scatterometer to enhance and validate the 3D performance of scatterometric measurements. Both systems are based on a microscope setup equipped with a special modified illumination scheme and with an additional lens, the Bertrand lens, to image the diffraction pattern, the so-called scatterogram, onto a CCD detector.

The PTB system has been equipped with a 543 nm HeNe laser as light source. The illuminating laser beam is focused at arbitrary positions in the entrance pupil of the microscope system to generate an approximated plane wave illumination with a well-defined but variable angle of incidence at the sample. This system has been set up and used to study and improve the 3D measurement capability on structures on wafers mainly for semiconductor industry.

The DFM system has been equipped with full pupil illumination creating a multi-angle illumination, which is much faster, but required a significantly more complex analysis of the measured integrated scatterograms. This system has been applied mainly to characterise diffractive structures.

Coherent Scanning Focused Beam Scatterometry

The inclusion of phase information in scatterometry is an additional source of information about the structures under investigation and was expected to enable another significant increase in parameter sensitivity and a further option to reduce the measurement uncertainties in scatterometry. Therefore, to have access to this phase information, the Fourier scatterometry method was improved at TU Delft by implementing a coherent illumination and scanning the focused spot. When the focused spot is moving along the periodic structure, the phase between the overlapping orders in the pupil is modulated. Since the scanning position of the spot can

be controlled using a piezo stage with high precision, the relative phase shift is also known. Involving the phase information into the fitting procedure increases the sensitivity of the measurement of the geometry parameters of the periodic structure significantly. This method can also be used for nanopositioning of the focused spot, because a shift even on the nanometer scale influences the interference pattern in the pupil significantly. In addition to extensive theoretical investigations of the potential of this method TU Delft has realised a corresponding measurement set-up. This system has been tested by comparison measurements at different 1D silicon gratings and its performance has been compared with classical scatterometry and ellipsometry.

3.1.2 Limitations and approximations in scatterometry

Systematic deviations are often observed for measurement comparisons between different scatterometer tools or methods as well as for comparison with microscopic (typically CD-SEM) results. These may be connected both to the applied measurement methods and tools, to necessary approximations in the modelling and data analysis and to imperfections and limitations of the target structures. Although these systematic offsets may also be at least partly attributed to the CD-SEM measurements or simply to inconsistencies in the definition of the measurands, for the implementation of scatterometry as absolute metrology (suitable also for quality control applications) it was necessary to identify, characterise and eliminate possible causes of systematic measurement errors and to evaluate thoroughly a complete measurement uncertainty estimation. Since data analysis in scatterometry is very cumbersome, for reasons of limited computational time and memory resources common approximations are usually applied to analyse the measurement data (e.g. the interaction area is generally supposed to be infinite in space). The illumination light is approximated to be a mono-frequent plane wave. However, in real systems a Gaussian beam (in the best case) with a finite spectral bandwidth is used. In addition, surface roughness and line edge and line width roughness are usually neglected, although the diffraction efficiencies are significantly affected by such roughness effects. To achieve traceability in scatterometry, the influence of each approximation has to be analysed and quantified thoroughly to develop an exhaustive and reliable uncertainty analysis.

Therefore, within this project we have investigated both numerically and experimentally the influence of some of these effects like the impact of varying spot size on the sample and the influences of existing line widths (critical dimensions, CDs) non-uniformity and line edge roughness on the scatterometric measurement results and we have tested possible size-dependencies of optical material parameters.

Finite spot size

Scatterometry test fields at production wafers are typically as small as $(50\ \mu m)^2$ and it is expected and planned in the near future that these field sizes will decrease considerably even further e. g. for so-called in-die measurements. Therefore, the illuminating beam is typically a focussed Gaussian beam in the best case with a diameter of a few 10 µm or even below. We have investigated by numerical simulations the deviation of the observed diffraction efficiencies for realistic Gaussian beams with varying spot size from the common results using a simple plane wave approximation. The Gaussian beams have been modelled either using a vectorial Gauss beam description or a plan wave decomposition description of the incoming beam. Additionally, we have investigated experimentally if there is a significant spot size dependence of the measured diffractions efficiencies by varying systematically the spot size in several steps between 40 µm and 1.6 mm. In the measurements down to 40 µm no significant spot size influence has been observed. This result is consistent with the numerical investigations predicting a significant deviation only below spot sizes of the order of 10 µm. As a result, for current tools and applications spot size effects are usually not significant. However, care has to be taken in the vicinity of Rayleigh resonances, where even for larger spot sizes of a few 10 µm observable deviation can occur.
In the future much smaller spot sizes (< 10 µm), e. g. for in die metrology, a realistic beam modelling will be required to avoid systematic measurement errors.

Size-dependent material parameters

For the complex refractive indices of the structure and substrate materials, homogenous values for n and k were assumed. However, for processed structures the values of these parameters are usually different from bulk materials and may be modified due to nano-structuring and possible quantum confinement effects. The observation of size-dependent material parameters has been reported in literature for MoSi line gratings on photomasks with periods well above 100 nm. Thus these values have to be measured independently or have to be fitted in the optimisation process. However, the latter is in general very hard or even impossible due to strong correlations e.g. between the k-values and the structure height. To study the possible interference

between structuring and other production parameters and the complex refractive index of the structure materials, different silicon gratings with varying line widths down to 25 nm have been measured and data has been analysed the data for an evidence size dependent material parameters. No evidence of size dependent material parameters has been significantly observed, so that for silicon (and similar manufacturing processes) this effect may be neglected. Gratings with much smaller line widths have not been available in sufficient quality.

Local structure roughness and non-uniformity

It is well known that line edge roughness (LER) and line widths roughness (LWR) may have a relatively strong influence on measurement results if not considered correctly in the data evaluation. In addition, LER and LWR as well as very low spatial frequency LER, the so-called CD non-uniformity, are important measurands in lithographic manufacturing of nanoelectronic devices. Therefore we have investigated the influence of such line edge irregularities on scatterometric measurements, developed methods to compensate for LER/LWR in the data analysis and developed and validated methods to characterise these important parameters reliably, accurately and with high statistical relevance by optical means.

The sensitivity on edge roughness is significantly enhanced for X-ray based scatterometry methods, as compared with scatterometry in the DUV or visible spectral range, in particular for edge roughness in the high spatial frequency regime. In this project we have tested and validated this sensitivity by numerical simulations and experimentally for EUV scatterometry and GISAXS. In particular GISAXS has proven to provide directly assessable information on structure roughness and long-range periodic perturbations. We have quantified by numerical simulations the impact of LER/LWR on goniometric scatterometry in the DUV, EUV and X-ray spectral range and we extended the currently available data analysis methods, such as the maximum likelihood method, to include LER/LWR as an evaluation parameter. With this approach it is possible to compensate for line roughness and additionally estimate the amount of LER/LWR directly from scatterometry data. Even from DUV scatterometry data we have been able to derive reliable estimates for the line roughness.

Additionally we investigated the measurement capability for CD-nonuniformity, i. e. variations of the line widths over a larger area or the full sample. For this purpose measurements on different test samples have been performed with EUV and DUV scatterometry, and have been compared with local probing AFM and SEM measurements. Figure 1 shows a typical result obtained on an EUV photomask. The agreement is usually quite good and demonstrates the suitability of scatterometry to characterise this important measurand. The observed remaining small deviations between the different tools may be attributed to small variations of the local edge profiles, such as varying rounding at the top or bottom corner of the edge.

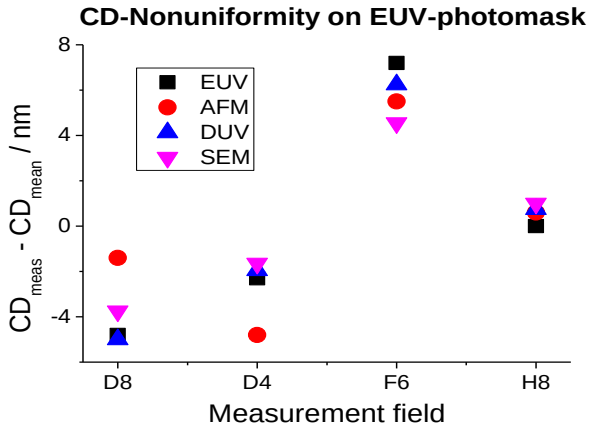

Figure 1. Measurements of the CD on different positions on a photomask using DUV and EUV scatterometry and comparison with results obtained by commercial AFM and SEM metrology tools.

3.1.3 Advanced data evaluation and statistical treatment

Advanced data evaluations to treat the statistical inverse problem in scatterometry have been developed and applied to measurement data. Several achievements improved data evaluation by increasing precision and accuracy of the reconstructed profile parameters. Moreover, associated uncertainties were calculated and discussed.

To solve the inverse problem we have introduced the maximum likelihood estimation together with a measurement error model. In contrast to simple least square fits, the maximum likelihood method estimates the parameters of the error model which yields the determination of accurate and precise geometry parameters. Uncertainties were estimated locally by the inverse of the Fisher Information matrix which presumes that the distributions of uncertain geometry parameters are Gaussian.

The evaluation of uncertainties by the Fisher Information matrix method has the disadvantage that uncertainties are determined locally and effects of multiple maxima are not taken into account. To study the

significance of that effect we compared the Fisher information matrix method with a simple Monte Carlo method. We sampled from a distribution of simulated measurements and reconstructed the geometry parameters by the maximum likelihood method. We applied both methods to two models, one with and the other without line roughness. Surprisingly, we found that the quality of the uncertainty estimation within the Fisher information matrix method depends on the model. In the model without line roughness, multiple local maxima appear and the local calculated uncertainty is too small. For the other model (including roughness) the estimates for the uncertainties are comparable for both methods. The Monte Carlo method provides reasonable estimates for both models, but is characterised by high computational costs.

3.1.4 Modelling of realistic geometries

In section 3.6 we illustrate the effect of line roughness on the reconstruction of grating parameters employing the maximum likelihood scheme. Neglecting line roughness introduces a strong bias in the parameter estimations. Therefore, such roughness has to be included in the mathematical model of the measurement in order to obtain accurate reconstruction results. We have extensively investigated three different models for EUV scatterometry at an EUV photo mask with increased complexity of the geometric structure model, by successively including two major sources of systematic errors, namely line roughness and deviations in the multilayer substrate of the EUV mask. Applying the different models to reconstruct the CDs from both simulation and measurement data, we have demonstrated the improvements of the reconstruction. Thus the refinement of the geometry model including more realistic structure parameters in the maximum likelihood approach to the inverse problem leads to a significant reduction of the variances in the derived CDs proving a reduction in the measurement uncertainty for scatterometry. In addition, the developed maximum likelihood method allows estimating mean values of line roughness directly from scatterometry. The approach was demonstrated for simulated scattering intensities and for experimental data of EUV and DUV scatterometry measurements. Results obtained from the experimental data have been shown to be in good agreement with independent AFM measurements.

In addition, we have investigated a 2D-Fourier transform method as a simple and efficient algorithm for stochastic and numerical studies to investigate the systematic impacts of realistic line edge roughness on light diffraction pattern of periodic line-space structures.

The key concept is the generation of ensembles of rough apertures composed of many slits, to calculate the irradiance of the illuminated rough apertures far away from the aperture plane, and a comparison of their light intensities to those of the undisturbed, 'non-rough' aperture. We applied the Fraunhofer approximation and interpreted the rough apertures as binary 2D-gratings to compute their diffraction patterns very efficiently as the 2D-Fourier transform of the light distribution of the source plane. The rough edges of the aperture slits are generated by means of power spectrum density (PSD) functions, which are often used in metrology of rough geometries. The mean efficiencies of the rough apertures reveal a systematic exponential decrease for higher diffraction orders if compared to the diffraction pattern of the unperturbed aperture.

The implicated model extension for scatterometry, by an exponential damping factor for the calculated efficiencies, allows determining the standard deviation σ_r of line edge roughness along with the critical dimensions (CDs), i.e., line widths, heights and other profile properties in the sub-micrometer range. First comparisons with the corresponding roughness values determined by 3D atomic force microscopy (3D AFM) showed promising results.

Besides FEM we have used also Finite Difference in Time Domain (FDTD) method for calculations of electromagnetic field distribution interaction with microstructures and nanostructures. For this, this we have modified and further developed the open source software *Gsvit* for FDTD modelling to address problems in scatterometry. This software is freely available on http://gsvit.net. Within this project, the main modifications of the software have been related to modelling of periodic structures, addition of random roughness to modelled objects, handling of general 3D geometries and setup of a graphical user interface to simplify access to the software for other partners (see Fig. 2).

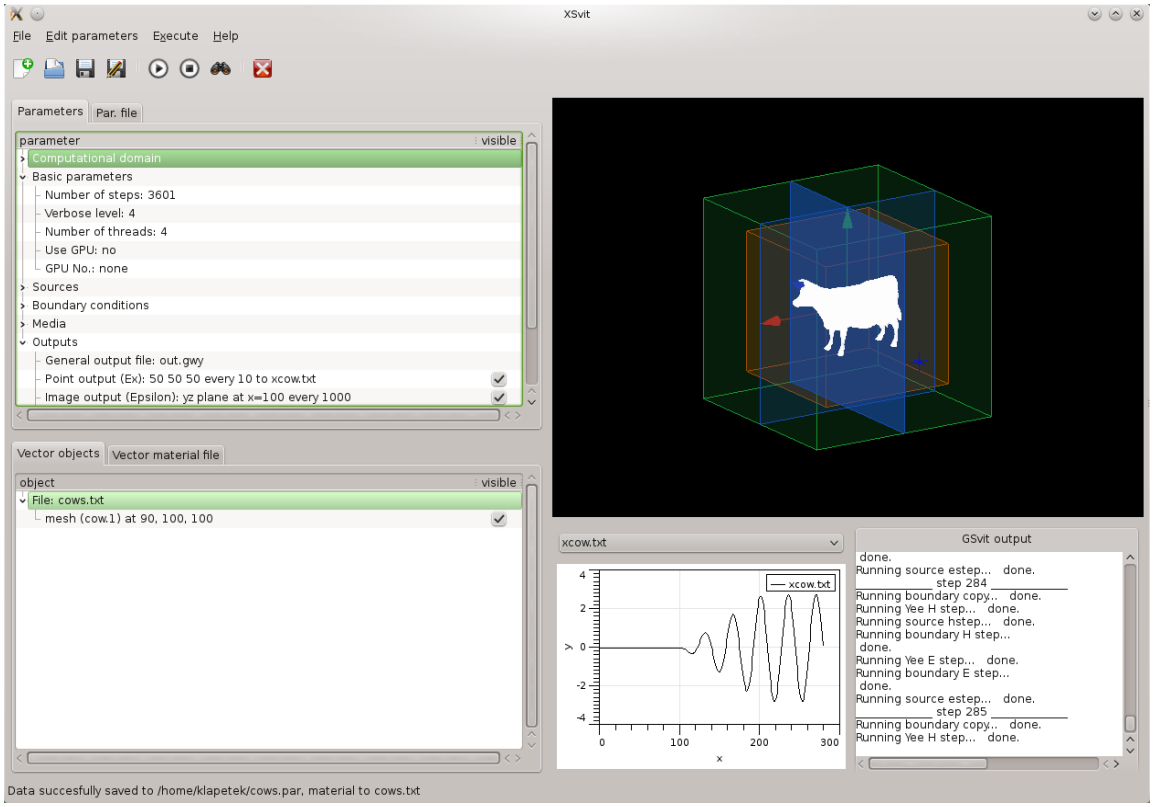

Figure 2. Graphical user interface of developed FDTD software

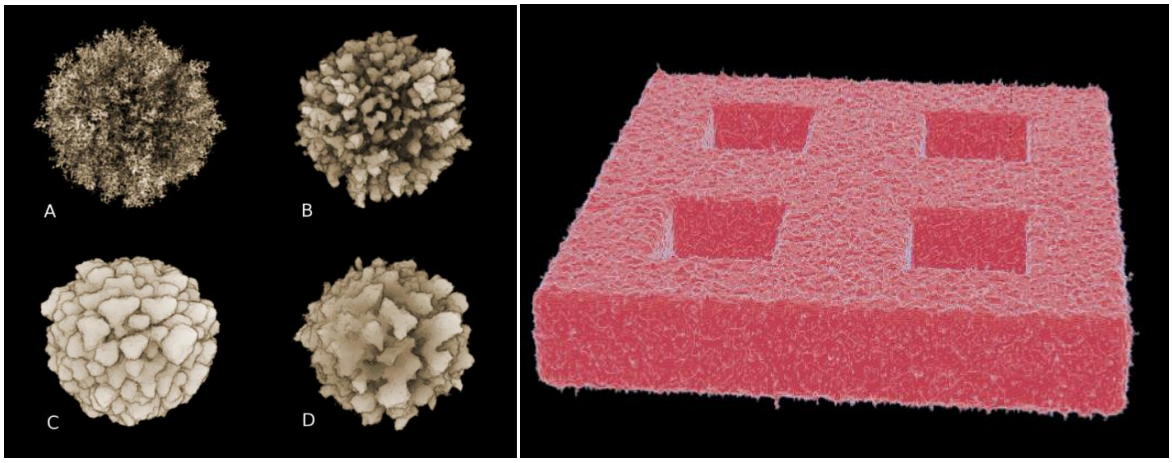

Figure 3. Application of random surface roughness on a sphere (left) and on reflection grating (right).

From the point of uncertainty analysis the most important part of the software are object modifiers that allow easily incorporating different surface irregularities into computational geometry and making the model closer to reality (see Figure 3). Three variants of object modifiers were created: random roughness, shadowing growth and arbitrary function. Using this approach we can add different classes of irregularities to any modelled object, from sinusoidal perturbation up to a fractal surface. Example applications of such random structures are shown in Figure 3.

3.1.5 Measurement comparisons of 1D gratings

To test and validate the performance of the different scatterometry methods and systems developed within this project and to compare the measurement results with state of the art microscopy methods, systematic measurement comparisons have been performed on different 1D grating structures. The aim of these

comparisons was to test the tool matching between different systems, to identify possible systematic measurement deviations and to evaluate and eliminate the reasons for such possible systematic deviations. Additionally, the specific parameter sensitivities for different tools and samples have been analysed. The final goal of these comparisons was to provide valuable information and guidance on i) optimal tool configurations, adequate modelling and data analysis, and on ii) traceability of the measurements to end users in industry and at the NMIs.

For these comparisons we selected three different samples, two silicon commercial wafer samples from different suppliers and one state-of-the-art chromium photo mask. These samples covered a parameter range from 300 nm to 1000 nm for the grating periods and 150 nm to 500 for line width. The nominal structure heights have been specified by the different suppliers to be 70 nm for the chrome mask and 315 nm and 345 nm for the two different silicon samples.

As main sources of systematic measurement deviations, we have identified: differences in the applied structure geometry models and insufficient knowledge on material compositions and optical material parameters, for Si structures in particular of the inevitable oxide layer. A sufficiently detailed and realistic structure model is a crucial precondition for reliable scatterometric measurements.

Table 1: Measurement results for a 1D Si grating, as obtained with coherent Fourier scatterometry, DUV scatterometry and Mueller polarimetry. DUV measurements have been analysed with two different methods, a conventional least square optimisation and maximum likelihood estimation including line roughness as additional fit parameter. The stated uncertainty values correspond simply to the 1σ uncertainty estimations derived from the nonlinear optimisation process and are not based on complete uncertainty budget estimations, and are therefore not providing realistic uncertainty estimations.

1D Si grating Eulitha AG, 600 nm pitch	CFS (TU Delft)	*DUV scatterometer (PTB)*		Mueller polarimeter (DFM)
		MLE	*least squares*	
midCD / nm	277 ± 1.5	*301.5 ± 1.5*	*277 ± 1.2*	287 ± 1.5
height / nm	365 ± 0.8	*361 ± 1*	*370.8 ± 0.5*	379.4 ± 0.8
SWA / degrees	86 ± 3	*83.8 ± 0.3*	*81.9 ± 0.2*	85.2 ± 0.8
Oxide layer thickness / nm	5 ± 0.2	*4.9 ± 0.5*	*2.77 ± 0.28*	8.0 ± 2.2
Line roughness / nm	-	*9.5*	-	-
top corner rounding / nm	-	-	-	0
bottom corner rounding / nm	-	-	-	71.1 ± 2.1

Table 1 shows a typical example of a non-ideal comparison: The least square analysis of the DUV measurements and the analysis of the CFS measurements are based on the same geometry model. Therefore, the agreement of these results is acceptable. However, if additional refinements of the structure model are added, as in this example a bottom corner rounding for Mueller polarimetry data or line edge roughness for the MLE evaluation of the DUV data, the resulting CD value is shifted by 10 nm and 24.5 nm respectively.

For the DUV measurements on this Si grating the requirement of a sufficiently realistic geometry model is clearly confirmed by the example shown in Figure 4: Here, the same measurements have been analysed with and without inclusion of top and bottom corner rounding. It is clearly observed that the inclusion of the bottom corner rounding dramatically improves the best fit results, whereas there was no significant hint for top corner rounding.

On the other hand this result demonstrates the capability of scatterometry to derive even small structure details such as bottom corner rounding, which is hardly measurable by other destruction-free methods.

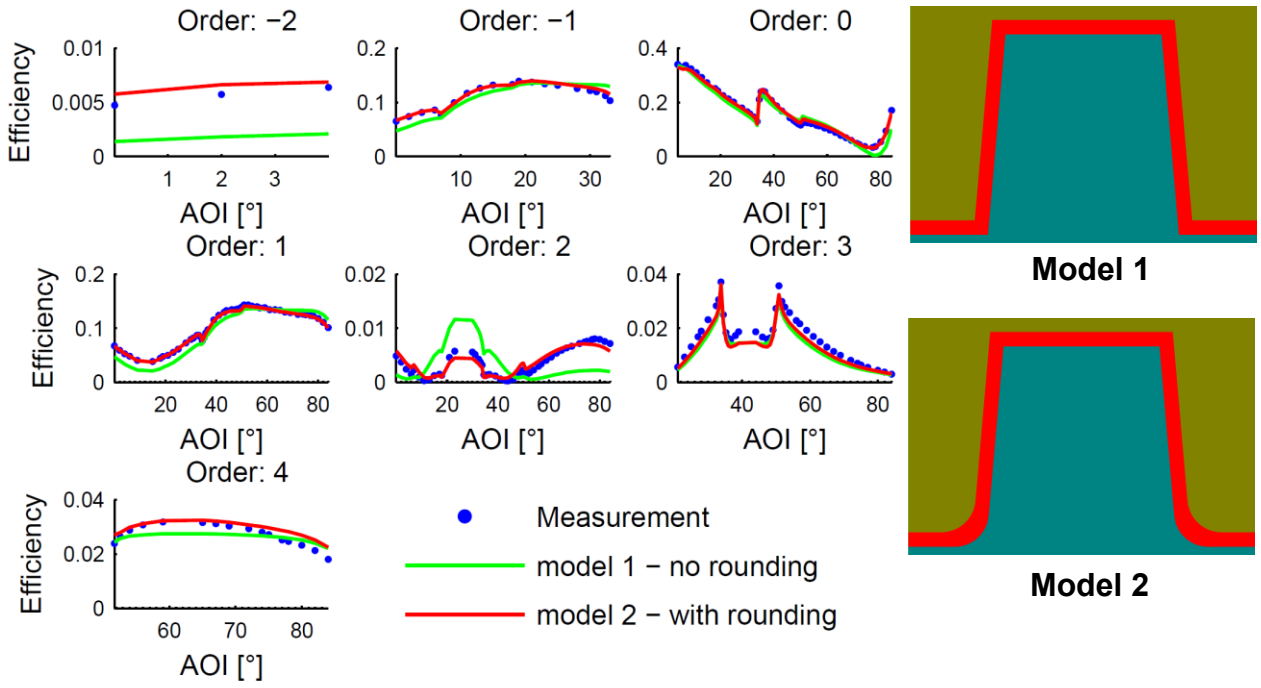

Figure 4. DUV scatterometry measurements at Si grating sample with 600 nm period (blue dots) analysed with two different geometry models: model 1 without and model 2 without bottom corner rounding; the improvement of the optimisation result using model 2 proves clearly the significance of this parameter

3.1.6 Modelling and data analysis of measurements of 2D gratings and 3D structures

A software module has been adapted (FEM solver for 2D and 3D light scattering simulations) and used in Matlab-scripts for performing inverse analysis of 3D scatterometry data by JCMwave in collaboration with PTB. The FEM solver allows for special features, improving performance for scatterometry simulations (parameter derivatives are computed fast and efficiently). The software module has been successfully tested and applied within this project.

Besides FEM we have used also the Finite Difference in Time Domain (FDTD) method for calculations of electromagnetic field distribution interaction with microstructures and nanostructures. We have investigated a 2D-Fourier transform method as a simple and efficient algorithm for modelling of 3D structures.

A limiting factor for the use of numerical methods in scatterometry in 3D is still the speed of computation. Therefore, many of the problems are being simplified using different symmetries. This approach is not always possible and a speedup of fully 3D calculations is desirable. To speed-up calculations using FDTD we have continued our effort to use graphics cards for the modelling. Graphics cards are very low cost and powerful computational tools available. As the FDTD algorithm is in principle well suitable for parallelisation, use of graphics cards can significantly improve FDTD performance, like shown in Figure 5. The option to use graphics card to accelerate rigorous FDTD modelling has been implemented to the freely available software Gsvit (http://gsvit.net).

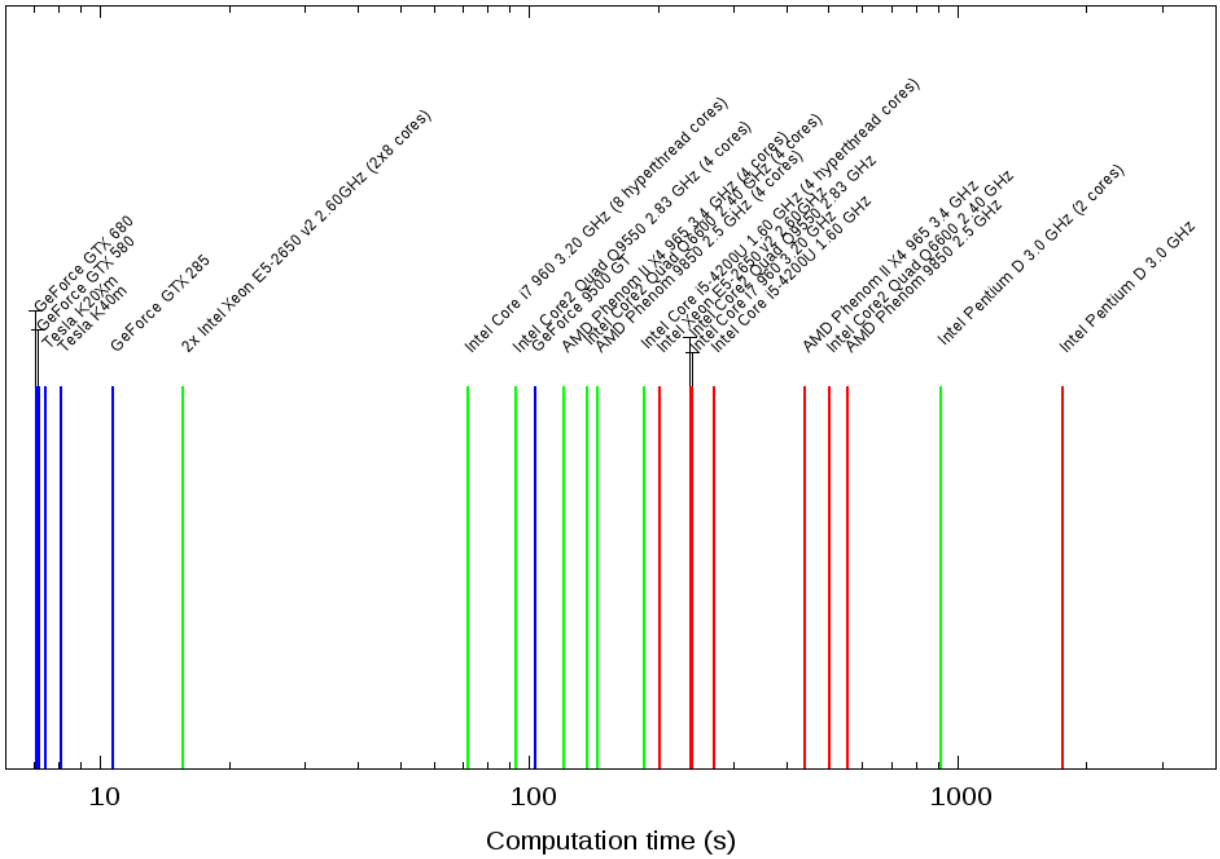

Figure 5. A reference FDTD calculation duration on different computer processors and graphics cards.

3.1.7 Measurements on 2D gratings

As test sample a hexagonal 2D Si grating with pillar structures was used (cf. fig 6 to 8). The grating was specified to have a nominal period of 600 nm, structure diameters of 317 nm, a structure height of 310 nm.

Reference measurement have been performed with PTB's high resolution DUV scatterometer within the 6 main diffraction planes and have been quantitatively analysed by rigorous FEM modelling (cf. Figure 7b). Additionally, microscopic reference measurements have been performed with PTB's 3D AFM and low voltage SEM. Figure 8 shows an example SEM measurement of the hexagonal Si grating. The 3D geometry of the grating structures have been measured and compared with each other and with the DUV scatterometry and GISAXS results.

a) b)

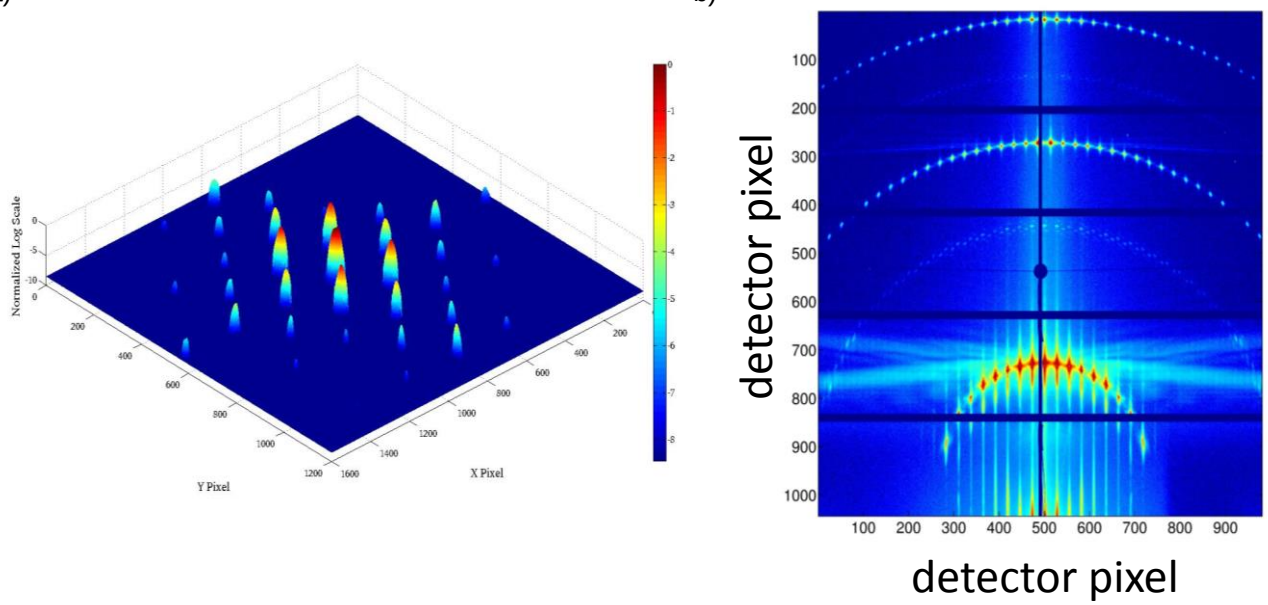

Figure 6. Measured diffraction efficiencies obtained with a) the Fourier scatterometer and b) the GISAXS system

a) b)

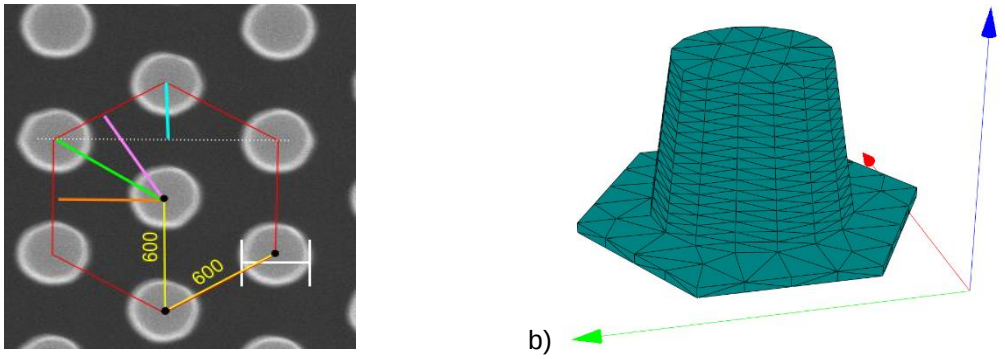

Figure 7. Scatterometric reference measurements with PTB's DUV scatterometer. a) the hexagonal 2D grating of silicon pillar structures can be measured in (at least) 6 different coplanar cross sections; b) FEM model of a pillar structure without oxide layer

GISAXS, DUV scatterometry and microscopy results show a reasonable agreement and confirm the principal suitability of GISAXS for the characterisation of 3D structures. For a final reliable quantitative evaluation of the results and the corresponding measurement uncertainties some more microscopic data for a statistically significant comparability is required, since the GISAXS measurements are evaluating (and require) a large interaction area of about 15 mm^2, which is huge as compared with the AFM and SEM sampling areas.

a) 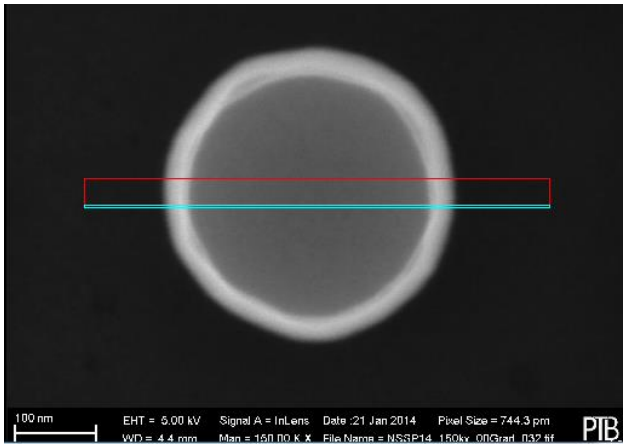

b) 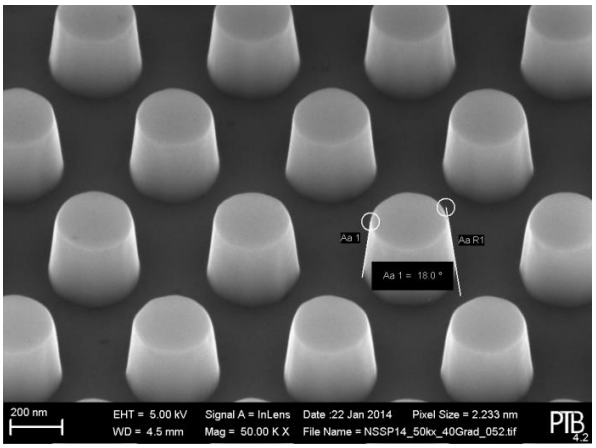

Figure 8. SEM characterisation of 3D structures: a) top down image of one pillar gives roundness deviation, top and bottom diameters and first edge angle estimations, b) series of controlled sample tilting allows to determine structure heights, edge profiles and an alternative approach for edge angle determination.

The measured diffraction efficiencies for the Fourier scatterometer show a reasonable agreement with numerical simulations. A quantitative evaluation of the data was not meaningful because so far this test setup has not been fully characterised. Instead, a high resolution 193 nm Fourier scatterometer is currently being set up and characterised at PTB. This system will enable high quality scatterometric 3D measurements in the future.

Conclusion

The impact of the main commonly applied approximations and simplifying assumptions on the measurement results have been evaluated and quantified enabling much more complete and reliable measurement uncertainty estimations. With this, significant reductions in the measurement uncertainties even for conventional scatterometry methods were achieved.

Novel methods such as Mueller polarimetry and Coherent Scanning Focused Beam Scatterometry have been developed and evaluated.

Our studies on advanced data analysis methods shows that the maximum likelihood method provides accurate and precise results for the reconstruction of geometry/error model parameters. The quality of parameter estimations and the values of associated uncertainties depend on the model used. There are models where the Fisher information matrix method is not appropriate. The Monte Carlo method recommended by the Guide to the expression of uncertainty in measurement (GUM) appropriately quantifies uncertainties for both models.

3D capability of scatterometry has been significantly improved by better modelling and scatterometry methods: Much faster algorithms in combination with parameterisation of 3D-problems are implemented in an efficient software module now available for analysis of 3D scatterometry data. Three different scatterometry methods for advanced 3D metrology, Fourier scatterometry, sectioning goniometric scatterometry and GISAXS have been tested and validated for 3D measurements and are available now.

With these results the understanding of scatterometric measurements has been significantly improved, essential possible sources of systematic measurement offsets have been identified and quantified and the sensitivity of scatterometry for different structure parameters has been increased significantly with the developed novel methods. Thus these results are a main contribution to the improvement of the traceability and accuracy of scatterometric methods from an uncertainty level of above 10 nm at the beginning of this project to a level of few nm for individual methods and to a level of about 1 nm, as demonstrated by the calibration results of the scatterometry standard described below in section 3.6.

3D capability of scatterometry has been significantly improved by better modelling and scatterometry methods: Much faster algorithms in combination with parameterisation of 3D-problems are implemented in an efficient software module available now for analysis of 3D scatterometry data. Three different scatterometry methods for advanced 3D metrology, Fourier scatterometry, sectioning goniometric scatterometry and GISAXS have

been tested for 3D measurements and are in principle available now. A quantitative validation of the Fourier scatterometry approach is pending but will be performed as soon as the 193 nm Fourier system is under operation.

3.2 Extension of scatterometric methods

Introduction:

To support the goals described in the previous section, we investigated and developed novel approaches of short wavelength scatterometry in the EUV to mid X-Ray regime to benefit from the short wavelength and correspondingly enhanced sensitivities for some structure parameters as compared with scatterometry in the optical spectral regime.

Diffractive optical elements can control light beyond the capabilities of traditional optical components, which enables their use in various photonics applications. Methods for a detailed characterisation and measurements of the elements are essential to i) understand the operation of the elements, ii) support the development of fabrication processes and iii) for quality control of the manufactured elements. Traditional methods are not optimally suitable for the task but scatterometry can break the barriers of the traditional methods enabling more detailed and in many ways better characterisation tools.

To enable scatterometry becoming a suitable metrology method to support the development and manufacturing of diffractive and hybrid optical components, different scatterometry methods have been investigated, modified according to the requirements of diffractive optical components and validated by measurement comparisons. For this purpose, a special set of test charts has been designed and manufactured within this project and the data analysis procedures have been adapted to the special requirements of these applications. In particular, within this project we have developed and tested two different methods, goniometric scatterometry and Mueller polarimetry. For validation we have manufactured and characterised different complex types of diffractive structures on planar substrates as well as on curved substrates as hybrid samples, and have compared the measurement results with microscopic measurements.

Discussion of results:

3.2.1 Short wavelength scatterometry

Optical scatterometry in the DUV and visible spectral range is to some extend limited in sensitivity, in particular regarding small structure details such as line edge roughness, because the wavelength is much larger than the structures to be investigated and thus only the 0th order of diffraction, the specular reflection or transmission, exist. Thus, X-ray scattering is investigated as a candidate to support future metrology for semiconductor industry at wafer level. An essential advantage of X-ray methods is the high sensitivity to structure features in quite high spatial frequency regimes, for example to edge roughness.

To further enhance the sensitivity and flexibility of the EUV scatterometry by exploitation of polarisation information within this project, PTB commissioned a new versatile Ellipso-Scatterometer which is capable of measuring 6” size mask substrates in a clean, hydrocarbon-free environment with full flexibility regarding the direction of the polarization of the incident light.

Even more challenging structures, however, are on the wafer level, where the grating periods are typically a factor of four smaller. For this reason, structured wafers have been one of the main focuses within this project. In contrast to EUV photomasks on wafers the measurement is not supported by a highly reflective EUV multilayer underneath the structures. However, in grazing incidence geometry (GISAXS), small angle X-ray scattering (SAXS) is also applicable for wafer samples, for thick samples and non-crystalline substrates. The photon energy can be adapted to the sample system, e.g. taking advantage of X-ray absorption edges to improve the contrast. At PTB, the available photon energy range extends from 50 eV up to 10 keV at two adjacent beamlines.

We investigated the feasibility of characterising silicon gratings with radiation in the spectral range from EUV to X-ray. As for DUV/VIS scatterometry the X-Ray measurements are simulated by rigorous modelling the interaction of electromagnetic radiation with the investigated structure. Furthermore, discrete frequency contributions in the diffuse scatter intensity can be correlated to process parameters of the e-beam writer used for the grating production.

Representative results for the GISAXS measurements are shown in Figure 9. The radiation was incident parallel to the grating lines. In this set-up the main diffraction orders appear along a circle which contains the specular reflection in the uppermost position. For the left example these orders clearly dominate the figure and only faint satellite orders are observed. For the right example a much higher exposure dose has been applied to make also faint satellites visible. These satellite orders appear throughout the field of our detector up to at least the 9th order, indicating a high periodicity of the structure. The placement of these satellite orders also nicely illustrates the different scales for the diffraction orders in x and y direction in the GISAXS geometry. The orders in the y direction correspond to the period of the measured grating of 100 nm, while the periodicity causing the satellite orders is 4.52 µm along the grating lines, i.e. x direction, indicating a periodic stitching error in the manufacturing process. The 4.52 µm period represents the smallest writing area of the e-beam lithography system.

The GISAXS instrumentation with the large in-vacuum Pilatus detector at PTB has the advantage of providing all information in a single shot. Due to the small diffraction angles of the GISAXS system, equipped with the image detector is in particular suitable to measure a large part of the conical diffraction patterns. Therefore this system is as well suitable for improved 3D characterisation of nanostructures.

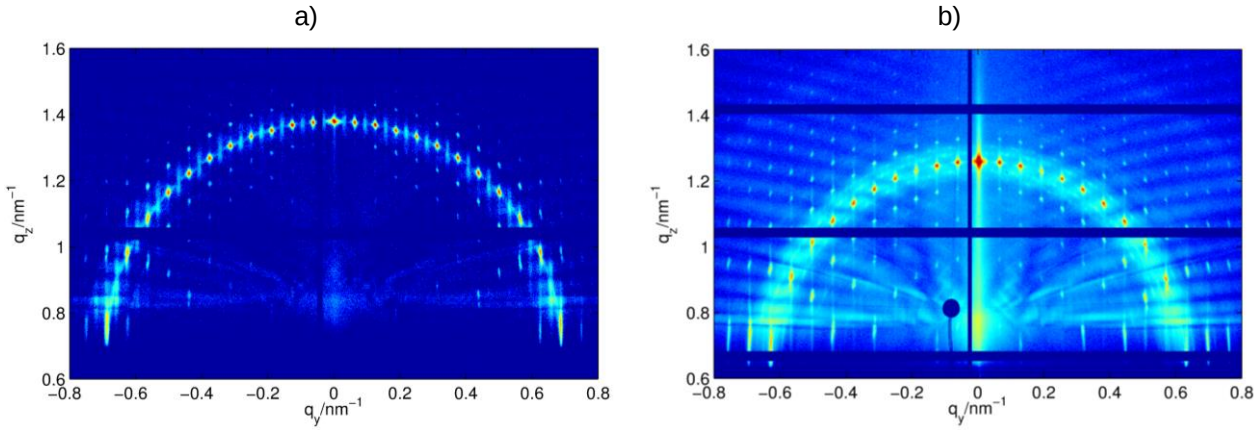

Figure 9. Typical results for GISAXS measurements. The intensities are represented on a log scale with false colours to show also satellites. Figure a) was taken with a short integration time. The circle with the main diffraction orders is dominating. Figure b) was taken with a long integration time to also resolve faint satellite peaks.

For lower photon energy we used the Ellipso-Scatterometer at the EUV beamline as well for small angle scatterometry (EUV-SAS). Here, a “single pixel” photodiode is used which is scanned across the trajectory where the diffraction orders appear. This scheme allows to measure at any angular orientation and thus to take advantage of the full available photon energy range.

3.2.2 Development of diffractive test structures on planar and curved substrates

To cover a large range of typical applications in the fabrication of diffractive and hybrid optical components, two sets of diffractive optical elements have been designed and fabricated at UEF in collaboration with Nanocomp, MIKES, and DFM. The first set contains binary gratings on a planar surface which are periodic either in one or two dimensions. The second set contains one dimensionally periodic binary grating on a curved surface. Both sets were fabricated on a silicon dioxide substrate.

The planar samples contain one dimensionally periodic binary gratings with four different periods: 300 nm, 500 nm, 700 nm, and 900 mm, with the fill-factor of 0.5 in all cases, and additionally a binary 1-to-5 beamsplitter with a period of approximately 6 µm. The first mentioned structures are easier to characterise because they contain only a few unknown parameters that describe the profile of the grating. The internal structure of the beamsplitter is more complex with higher number of unknown parameters and thus is more challenging to characterise with optical methods. The 2D periodic elements differ from the 1D counterparts by much larger period and more complex internal structure. The first is a cross generating element and the second creates a random dot matrix both including several hundreds of diffraction orders. Because of the large period, the

angular separation of the diffraction orders is very small which creates a challenge for the measurement setup. The height of all gratings on a planar surface is 675 nm.

The designed period of the binary grating on a curved surface is 500 nm with the fill-factor of 0.5. The curved substrate itself is of sinusoidal form with the period of 20 µm and the height of approximately 600 nm. The height of the binary grating varies along the sinusoidal surface such that the height is 800 nm in the valley and approximately 200 nm on the top of the surface. The sinusoidal structure was also fabricated without the grating for comparison.

3.2.3 Goniometric scatterometry for diffractive structures

In this project, MIKES has developed and built a goniometric scatterometer to address the needs of manufacturers of diffractive optical elements in Europe. The work has included the design, realisation and metrological characterisation of the measurement setup. The system can be used with different illumination wavelength between 405 nm and 633 nm and the detection unit has been equipped with lock-in technique to enhance the signal-to-noise-ratio. The work has been done in close collaboration between MIKES, UEF and Nanocomp. As an industry partner, Nanocomp has clearly stated the needs of the diffractive optics industry and added the industrial insight into this development, and UEF has supported and improved the data analysis.

To obtain the geometric parameters from measured diffraction efficiency data, the inverse diffraction problem has to be solved by using rigorous electromagnetic methods and conventional optimization algorithms. For this, we have applied the Fourier Modal Method (FMM), also known as Rigorous Coupled Wave Analysis (RCWA). The reconstructions have been performed in UEF. The reconstructed parameters were obtained with the help of Nelder-Mead Simplex algorithm using the design parameters as an initial guess. The uncertainties have been determined by Monte Carlo analysis using typically observed values for the standard deviations of repeated measurements of approximately 0.4%.

3.2.4 Mueller polarimetry for diffractive structures

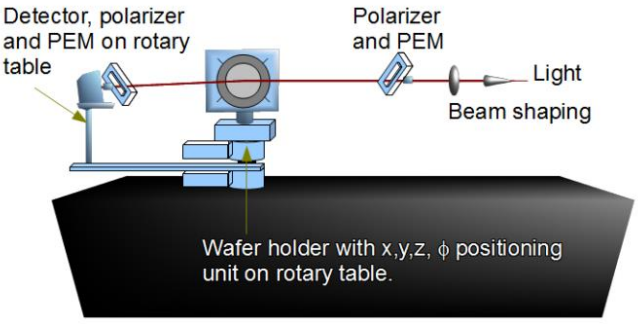

Figure 10. Illustration of the experimental Mueller Polarimeter setup at DFM.

At the beginning of this project DFM has had an angular Mueller Polarimetry setup using lasers as excitation sources in use, which showed some issues, in particular when analysing curved substrate samples. To solve these problems DFM decided to rebuild their instrument and analysis software such that the samples could be thoroughly investigated (c.f. Figure 10). This involved the following activities:

- Change the measurement setup and analysing software such to enable doing Mueller Polarimetry measurement in transmission.
- Change the instrument from an angular Mueller Polarimetry setup using laser excitation sources to a spectroscopic Mueller Polarimetry setup using a broadband xenon lamp as excitation source. This change involved building a complete new detection setup consisting of a monochromator, photomultiplier and a home-built amplifier for the photomultiplier.
- Change the analysis and instrumental software to handle spectroscopic Mueller Polarimetry data
- Calibrate the instrument using reference samples.

The modelling of the structures was done using software developed at DFM using the RCWA algorithm. For the reconstruction of the diffractive structures we used a developed least square software for Mueller Polarimetry with error propagation estimation and uncertainty analysis, called DFM-LSQ. In the reconstruction, the experimental data were fitted to the RCWA model structure.

This method and system has been tested for applications both on the planar and curved diffractive test samples, as described below.

3.2.5 Characterisation and measurements on planar diffractive optical elements

All planar test structures have been measured by goniometric scatterometry and Mueller polarimetry.

The measurement of the intensities of the diffraction orders gives the manufacturer a significant amount of valuable information. When analysed with numerical tools one can obtain very detailed information of the microscopic structure of the elements.

The reconstructed parameters were compared with measurement results obtained with AFM and SEM. The parameters of the binary grating, obtained by the scatterometric method, were very close to the values determined from AFM and SEM measurements. The results for the beamsplitter were also rather close to the corresponding values of the direct measurements but greater errors were obtained in some parameters. The reason for this is the more complicated internal structure of the beamsplitter for which the model may have been too simple. This complex structure also requires larger amount of measured data than simple structures to obtain a unique solution.

The approach has been tested with very simple diffractive elements generating only several diffraction orders and with significantly more complex structures, where not only the number of diffraction orders is higher, but the intensity pattern has been further adjusted by adding extra features to the microscopic structure. The measurement of those tiny features is very challenging and for some cases even impossible for the traditional methods, but it is rather straightforward for the scatterometric approach.

The microscopic structure of fairly simple structures can be easily and very effectively obtained by the approach. Although the characterisation of more complex structures requires more measurements and the numerical analysis is much more challenging, it is still possible to solve the structure with fairly good accuracy as confirmed by comparison with microscopic measurements.

3.2.6 Characterisation and measurements on curved diffractive optical elements

It has proved a very challenging task to investigate the curved diffractive elements manufactured at UEF with Mueller polarimetry and scatterometry for the following reasons:

1. Diffractive Optical Elements (DOE) are transmission objects, whereas Mueller polarimeters are usually designed as reflection technology.
2. In transmission objects like DOE strong coherence effects from multiple reflections may occur that give rise to unwanted ghost signals in the measurements.
3. The curved sample structure is much more complex than the problems usually considered in scatterometry.

The model for these calculations was based on manufacturer's information regarding the design shapes shown as the left picture in Figure 11. The long pitch and the advanced structure make it necessary to use a very large unit cell (called a supercell) with a very high number of diffraction orders (~200) to obtain stable numerical results. The final result was a very fast calculation time for the model structure; one calculation took less than 15 seconds CPU time on a computer with 2 CPUs and 4 cores.

For the reconstruction of the diffractive structures we used a especially developed least square software for Mueller Polarimetry with error propagation estimation and uncertainty analysis, called DFM-LSQ. In the reconstruction, the experimental data were fitted to the RCWA model structure and we obtained the result shown in Figure 11. The shape of the diffractive structures reconstructed from the Mueller polarimetry measurements have been very different from the initial design model. However, an AFM reference measurement confirmed the Muller polarimeter results, and with it the suitability of this tool and set-up to

characterise even such complex hybrid structures reliably. In conclusion, we have for the first time demonstrated reconstructions of such advanced DOE structures using Mueller polarimetry.

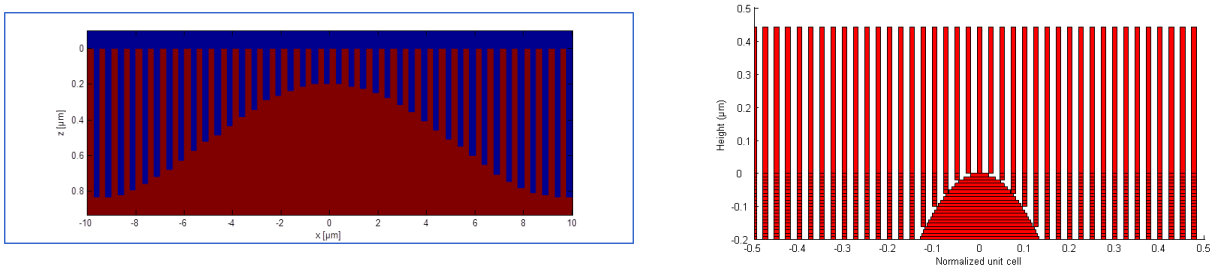

Figure 11. Illustration of the model structure of the DOE given by UEF(left) and the reconstructed structure (right). Both pictures show a supercell of the structure, defining the repeated unit cell with a pitch of 20 µm. In the right axis we use normalized unit cell e.g. the x-axis is divided with the supercell pitch. The y-axis zero point for the two pictures is located at different positions.

Conclusion:

Novel X-ray scatterometry methods such as GISAXS and EUV-SAS have been developed and evaluated. The high metrological potential of x-ray scattering methods, in particular, have been demonstrated and GISAXS is available now as a reference metrology of highest sensitivity and accuracy.

Scatterometry metrology solutions are available now for the first time for the optics industry to characterise fast and efficiently diffractive and hybrid (i. e. diffractive-refractive) structures and to support the manufacturing process. Two methods based on goniometric scatterometry and Mueller polarimetry have been successfully tested on different diffractive samples on flat and curved substrates and are ready for applications in optics industries, now.

3.3 Development of ultra-high resolution microscopy (AFM, SEM) to support scatterometry and to enable measurements comparisons with scatterometry

Introduction:

In addition to scatterometry, high resolution microscopy such as SEM and AFM are commonly applied to characterise the produced structures both for nanoelectronic and in diffractive optical devices. As local probing techniques, these microscopy methods are the methods of choice for characterising local structure details such as local edge profiles and edge roughness. Moreover, SEM is widely used for linewidth metrology in semiconductor industry (CD-SEM) and commonly used as CD reference system. A comparison with high resolution microscopy metrology systems have also been recommended to validate and compare both the capability to characterise the main measurands such as structure width (CD) and the sensitivity to further detailed structure features such as line edge roughness. However, AFM is usually a very local and slow probing method, and special modifications, extensions and statistical data analysis schemes had to be applied to enable a statistical relevant comparison with scatterometric measurements, which measure integral over a relatively large interaction area.

The comparability of local probing microscopy methods, which are usually limited to quite small measuring ranges, and the integral measuring optical methods is typically quite difficult. This is very likely often a reason for observed systematic differences between measurement results obtained with these methods. Thus, to compare microscopy and scatterometry on a statistically significant basis, long range microscopy methods and well defined sample strategies are required.

Discussion:

Such a long distance AFM with well adapted sampling strategies and a versatile and calibrated SEM has been used by PTB to provide the mentioned microscopic comparison measurements. Additionally, VSL has investigated and developed a novel long-range AFM for real 3D measurements. Finally NPL and PTB have developed a novel long-range AFM coupled to an X-ray interferometer to test with upmost accuracy local pitch variations of the investigated grating structures, in particular of the scatterometry standards developed within this project, and to enable a very accurate and alternative route to enhance the traceability in scatterometry.

3.3.1 X-ray coupled AFM

Within this project, we have worked on the development and realisation of an AFM coupled to a separated crystal x-ray interferometer, which was to be used as a high resolution translation stage that would provide traceable displacements of the sample under investigation. The x-ray interferometer (XRI) can be regarded as a ruler or translation stage were the spacing between graduations or the size of the translation steps of the stage are based on the lattice parameter of silicon that is traceable to the definition of the metre.

The interferometry is realised by diffraction of x-rays from the (220) planes in the interferometer which have a lattice spacing of 0.192 015 497 nm ± 1.2×10^{-8} nm, at 22.5 ◦C and a pressure of 1 atm. A design for the platform for the combined instrument was produced and is shown in Figure 12. An AFM was designed and constructed (Figure 13) that used a fibre interferometer for detection of the cantilever motion. Software was written for the operation of the AFM and the Plane Mirror Differential Optical Interferometer that was constructed and integrated into the AFM to provide traceable measurements of height of features measured in the AFM.

A novel long range translation stage for use with the x-ray interferometer was designed and constructed (Figure 14). The design was based on the use of cross flexure hinges and went through several iterations. When assembled, the stage had some angular errors at the arc second level. These were attributed to the cross flexures. Closer examination showed that it was possible to reduce the errors by adjustment of those cross flexures. However, it was necessary to individually measure the spring constants and out of axis motion of each of the flexures individually in order to determine the optimum orientation of the flexures and hence reduce the angular errors to an acceptable level. This was not completed by the end of the project. A modified version of the plane mirror differential optical interferometer was produced for use with the x-ray interferometer.

A goniometer system for the x-ray interferometer was constructed and software for the control written. A first version of the combined angle and displacement interferometer was manufactured. It was not possible to align the x-ray interferometer to the optical interferometer as the optical mirrors on the x-ray interferometer were of insufficient quality. At the end of the project a second x-ray interferometer had yet to be produced.

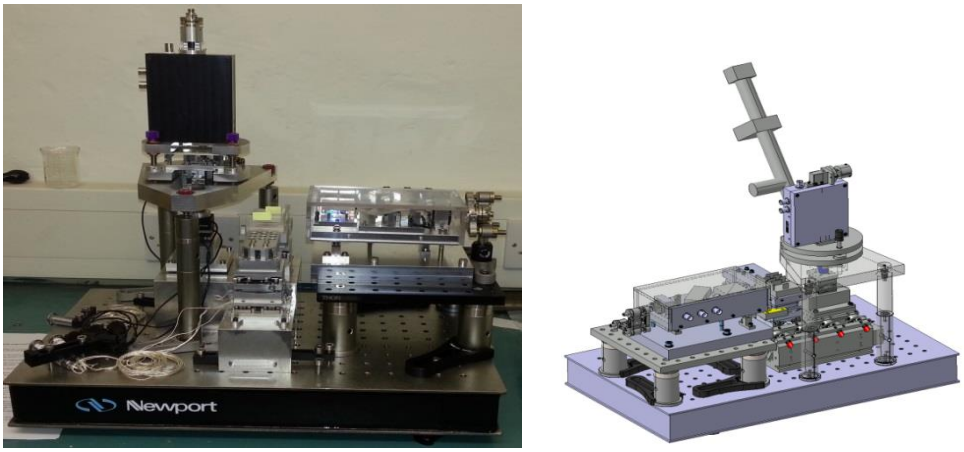

Figure 12. Photo and CAD drawing of the combined XRI optical interferometer and AFM

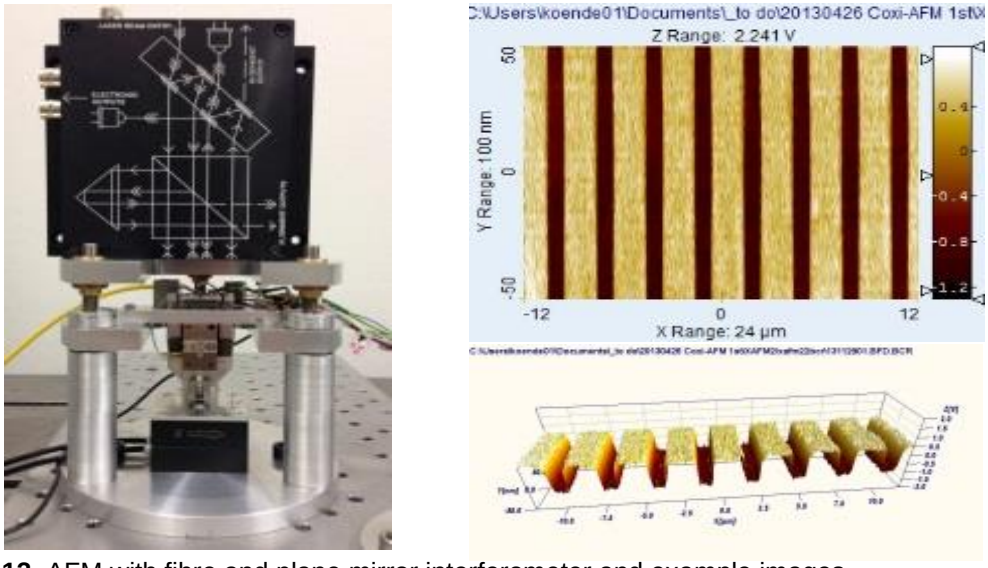

Figure 13. AFM with fibre and plane mirror interferometer and example images

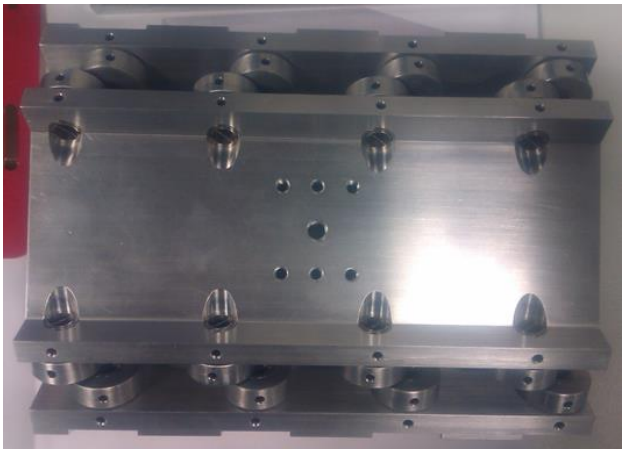

Figure 14. Long range (4 mm) translation stage for XRI

Considerable effort was directed towards the design of a new x-ray collimating device to improve the intensity of the x-ray signal from the interferometer. A collimating optic was designed and the order placed with a company that produced three versions of the optic.

This instrument was not complete at the end of the project. However, it will be completed in 2015 and will provide an excellent tool and reference for scatterometry and will be available for pitch calibration of the scatterometry standards with an outstandingly low measurement uncertainty.

3.3.2 Long-range 3D AFM

The aim of this work was to develop long range 3D-AFMs for traceable and accurate measurements of dimensional properties of nanostructures, whose data can be applied to support the modelling as well as to cross check and verify scatterometric methods. Within this project, two long-range 3D AFMs have been developed, both at PTB and at VSL.

The AFM at PTB uses the so-called scanning sample principle, i.e. the sample to be measured is scanned while the AFM head is kept stationary. In the instrument, the sample is fixed on a piezo stage, which is in turn mounted on the mirror corner of a large range mechanical stage (referred to as a nanopositioning and nano-measuring machine, NMM). The mirror corner is moved by stacked mechanical x-, y- and z-stages, which have a motion range of 25 mm, 25 mm and 5 mm, respectively. Three interferometers and two auto collimators measure the six degree of freedom of the mirror corner with respect to the metrology frame. By servo controlling the position and angles of the mirror corner, the NMM can position with nanometre accuracy.

Also the AFM concept at VSL features a scanning sample and a stationary AFM probe. For the sample movement a compact, high-stiffness, 3D translation mechanism is used, with a scanning volume of 1×1×1 mm^3. The motion of the stage is performed by Lorentz actuators and measured real-time by three laser interferometers, providing traceability to SI in closed-loop control. An additional benefit of the large scanning volume is that no additional coarse approach motors are required to bring the AFM tip and sample into close proximity.

Both AFM concepts normally operate in dynamic mode. In this mode AFM cantilever is commonly oscillated near the frequency of the first bending mode, which leads to sensitivity in the direction perpendicular to the

sample under investigation, but not in the in-plane directions. Hence, an AFM image thus obtained is not truly 3D, as for example information on the sidewalls of structures is lacking. To achieve 3D sensitivity both at PTB and at VSL higher order vibrational modes of AFM cantilevers are being used.

The PTB 3D concept uses the first bending mode and torsional mode to achieve both in-plane en out-of-plane sensitivity. Both modes are excited simultenaously using shaking piezos. The amplitudes of vibration are recorded using optical-beam deflection. Also the VSL concept relies on the bending and torsional modes of the AFM cantilever, but there are a few differences. First of all, a third mode is used to achieve sensitivity in the remaining in-plane direction, i.e. perpendicular to the torsional movement. To achieve this a vibrating element is created around the tip by removing material from a standard cantilever using focused ion beam milling. This substructure can oscillate independently from the cantilever. The three modes (bending, torsional, substructure) can be excited simultenously using photo-thermal actuation, in which the motion is realized by using an amplitude-modulated laser. This type of actuation is required, as with the more common piezo actuation it is impossible to excite the substructure mode. An additional benefit is the ability to combination of large amplitude and high bandwidth excitation. Also the VSL concept uses optical-beam deflection detection, resulting in an all optical solution(see Figure15).

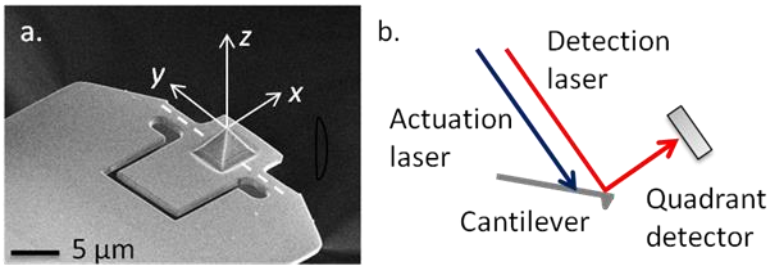

Figure 15. (a) Electron micrograph of a cantilever with a substructure machined around the tip. The axis of rotation of the substructure is indicated by the dotted line. (b) Scheme for photo-thermal actuation and deflection read-out using two lasers.

Another approach to 3D AFM, as developed at PTB, relies on a novel probing strategy, referred to as “vector approaching probing” (VAP). A VAP measurement process can be divided into three phases as shown in Figure 16. The first is the approaching phase. In this phase, the tip is moved towards the surface at a desired velocity vp (for instance 500 nm/s ~ 1000 nm/s) and the tip sample interaction is monitored in real time. The first phase ends once the tip sample interaction reaches a pre-defined status ST1. The second is the probing phase. In this phase, the tip is moved towards the surface until another pre-defined status ST2 is reached. Then the tip is withdrawn immediately from the surface until the tip sample interaction reaches again the status ST1. During the second phase, the x, y and z position of the nanopositioning stage and the sample interactions are recorded in real time and stored in the buffer of a digital signal processing (DSP) system. The third is the positioning phase. In this phase, the tip is moved to the next measurement point. Compared to conventional scanning AFMs where the tip is kept continuously in interaction with the surface, the tip sample interaction time using the VAP method is greatly reduced and consequently the tip wear is reduced.

The developed AFMs have been successfully applied for measuring a number of nanostructures in the frame of the project. Some detailed measurement examples will be demonstrated in the next section.

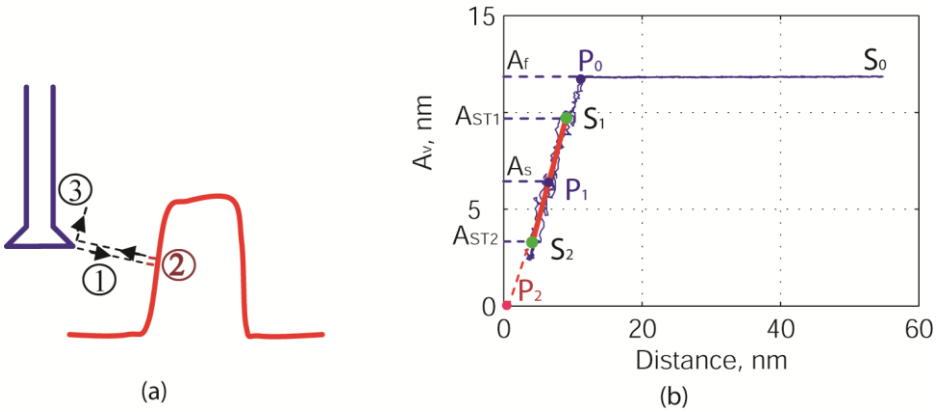

Figure 16. (a) Principle of the "vector approach probing. (b) A typical probing curve.

3.3.3 Testing of structure details using AFM and SEM

Two different AFM techniques, the CD-AFM and the tilting-AFM, have been developed and applied to measure structure details. CD-AFM uses flared tips, which have an extended geometry near its free end which enables the probing of steep and even undercut sidewalls, as shown in Figure 17 (a). The CD-AFM technique has advantages of measuring both the left and right sidewalls of nanostructures in only one measurement. However, it has disadvantages such as the relatively large tip geometry (typically tens to hundreds of nanometres) which limit its spatial resolution for measuring very dense structure patterns, and the complicated tip shape which makes the tip characterisation more difficult.

Tilting-AFM further extends the measurement capability of the CD-AFM. The advantage of tilting-AFM is its capability of applying very fine conical tips, for instance, super sharp silicon tips with a radius down to 2 nm, which offers better capability for measurement of dense structure patterns as well as for the corner rounding and footing of structures. But the tilting-AFM has its own limitations. In order to make the sidewalls of steep structures measurable, the AFM tip has to be tilted with respect to the structure by a certain angle, as shown in Figure 17 (b). As only one side of the structure is measurable at one tilted setup, either the AFM tip or the sample must be rotated so that the opposite side of the structure becomes measurable. Consequently, the images obtained at different tilting views must be stitched together to determine the CD, where the stitching error will strongly influence the measurement accuracy. Therefore, both AFMs were used in a complementary manner in this project, adding their strengths and overcoming their limitations, and thus reducing the measurement uncertainty and expanding the metrology versatility.

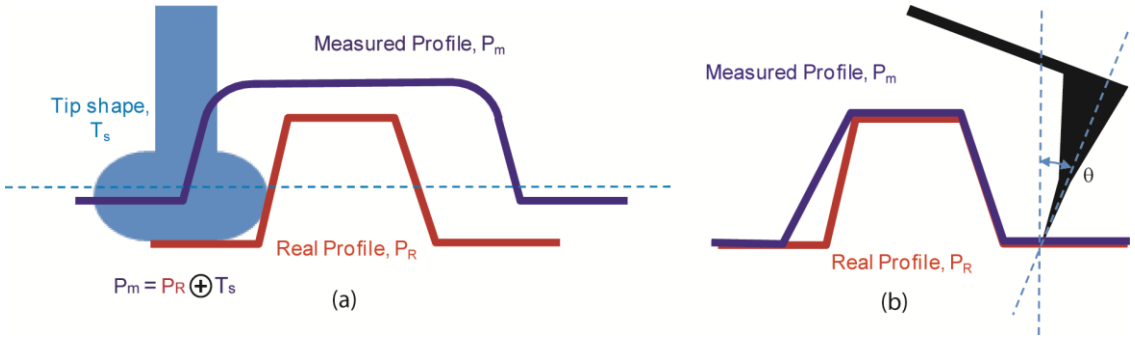

Figure 17. Principle of the CD-AFM (a) and tilting-AFM (b) applied in the measurement.

Both techniques were realised in a self-made AFM at PTB. This AFM uses the classic optical lever technique to detect the bending and torsion of the cantilever. AFM measurements are mostly performed in the intermittent-contact mode, where the amplitude modulation technique is applied for detecting the tip sample interaction. For achieving better CD measurement performance, new probing and measurement strategies have been developed. For example, the tip is capable of probing surfaces with a vertical and/or a torsional oscillation to enhance the 3D probing sensitivity; a "vector approach probing" method has been applied for

enhancing the measurement flexibility and for reducing the tip wear as well. The tilting-AFM is an add-on function of the existing instrument, which enables to apply a new type of AFM tips and manually tilting the scanner (together with the AFM head), while all other components including the controller and software are kept the same. The tilting angle is currently about 11 degrees in the tilting-AFM setup. In addition, to traceably calibrate the effective tip geometry, microscope TEM based method is applied, which uses either the silicon crystal lattice or the structure pitch value calibrated by metrological AFMs as an internal scale.

A large number of measurements on various specimens have been carried out, as demonstrated in Figure 18. The measured three dimensional structures details (such as height, sidewall angle, corner rounding, footing) are input to and for comparison with scatterometry. In addition, these tools have provided AFM measurements for comparison both on 1D and 2D gratings as well as for the developed scatterometry standards, as described below. Such comparison not only verifies the tools with each other, but also offers measures for understanding unknown systematic measurement errors.

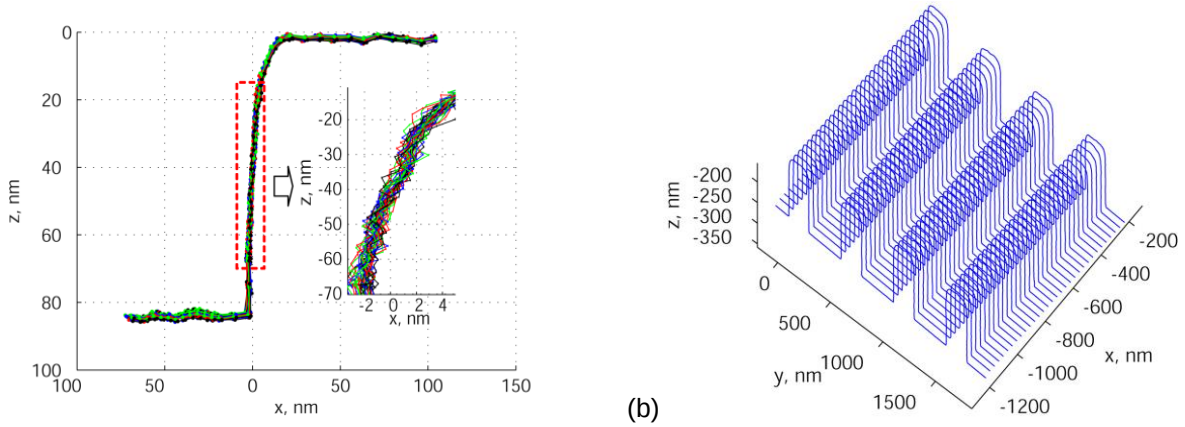

Figure 18. (a) Edge profiles of an EUV photomask line feature measured by the tilting-AFM using a super sharp AFM tip. Totally 32 repeated measurements by the tilting-AFM are plotted, showing excellent measurement repeatability. The inset figure shows the zoom-in details of the sidewall at the marked area; (b) measured AFM image using vector approach probing.

In addition PTB has used a commercial low voltage SEM (Zeiss Leo Supra 35VP) for the characterisation of structure details and comparison measurements. This system has a sample stage with well-defined tilting option to enable multi-angle measurements e. g. for characterisation of 3D structures. The scanning range is calibrated in-situ by means of calibrated grating standards.

Figure 19 shows a measurement example on a 1D Si grating and the analysis of edge positions, linewidth and further edge details such as top or bottom edge position corresponding to the local edge angle. For this purpose, a special edge detection algorithm recently developed at PTB has been applied.

Conclusion

Unique atomic force microscopes have been developed and investigated with promising outstanding features, such as long range 3D capabilities, to enable statistically relevant comparisons with the integral measuring scatterometry methods both on structure detail measurements such as edge roughness and on the main structure parameters CD, edge angle and height.

Both AFM and SEM measurements have been performed to support and validate the scatterometric methods, developments and measurement results. In particular, AFM measurements have been investigated to provide information on local structure parameters. These have been used to be utilised as *a-priori* knowledge about the structures to be measured to support the analysis of scatterometric data, and to validate the capabilities of the different scatterometry methods to derive these structure parameters directly from the optical measurements. Additionally, AFM and SEM have been included in systematic measurement comparisons of

nanoelectronic and diffractive optical structures to test and compare the performance of the different methods and systems in particular for CD metrology.

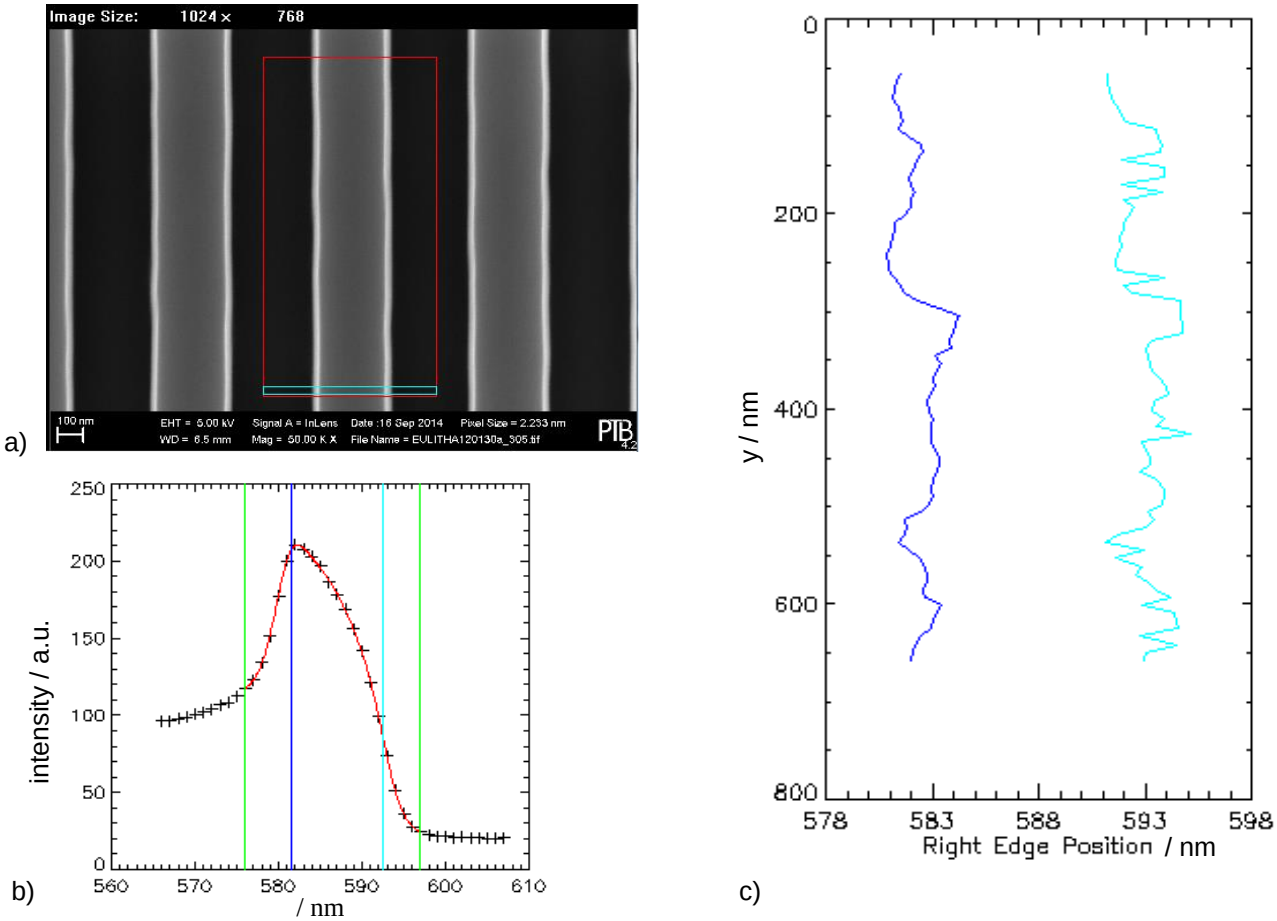

Figure 19. a) high resolution SEM image of a 1D Si grating b) analysis of edge positions applying PTB's so-called BDF-edge detection algorithm, c) top and bottom edge position versus scanning position applying the BDF analysis

3.4 Development of efficient and reliable methods for a combined data analysis of the different metrology methods

Introduction

Any scatterometric as well as microscopic metrology method investigated and applied within this project for dimensional measurements of nanostructures shows different sensitivity characteristics with respect to the different structure parameters. For this reason, the combination of different methods such as e.g. classical scatterometry, X-ray scatterometry and AFM combining the individual strengths of each method is a very promising route to achieve more reliable and accurate measurement results. Moreover, a combined analysis of data from different measurements applying adequate sophisticated statistical approaches allows to improve the traceability and to achieve measurement uncertainties significantly beyond the simple addition of the individual results. Therefore, we have developed improved mathematical methods for statistical inverse problems based on Maximum-Likelihood estimation and the Bayesian approach, and have applied these methods in different steps of combined data analysis:

- Use of *a priori* information e.g. delivered by AMF or SEM measurements or also design/manufacturer data to obtain improved MU determination of an individual scatterometric method

- Combined scatterometry data (e. g. DUV and short wavelength scatterometry or polarimetry), investigating different sensitivities to different structure parameters

- improved MU by combined data analysis of scatterometry and microscopy (AFM, SEM).

The goal for the different steps of MU improvement is a significant reduction as compared with the previous step.

As already mentioned in section 3.1, enhanced sophisticated mathematical data analysis methods have been required to enable the determination of reliable and complete measurement uncertainty considerations for all methods considered. This is even more important when combining distinct advantages of different scatterometric methods in a hybrid metrology approach supported by sophisticated combined data analysis methods.

Discussion

As already described in section 3.1, to solve the inverse problem, we have introduced the maximum likelihood estimation together with a measurement error model. The uncertainties were estimated locally by the inverse of the Fisher Information matrix which presumes that the distributions of uncertain geometry parameters are Gaussian. This maximum likelihood approach already allows realizing a simple combined data analysis of two measurement systems, if the measurement results of both systems show a Gaussian probability distribution. Also in section 3.1 we described the influence of line edge roughness on the results and uncertainty evaluations using both the Fisher information matrix method and a simple Monte Carlo method. For Gaussian prior knowledge distributions, we developed an algorithm to approximate the likelihood function and in turn the posterior distribution. From these results we derived a modified likelihood function, which allows including of line edge roughness data obtained e.g. by AFM or SEM measurements (c.f. sections 3.4.3 and 3.6.3). The scheme was applied to combine consistently EUV scatterometry-data and AFM measurements. AFM measurements are used as prior knowledge. It was demonstrated that the combination of both measurement techniques reduced the overall uncertainties which are given as credible interval of the posterior distribution. As an example, Figure 20 shows reconstruction results for the parameter sidewall angle SWA without and with inclusion of realistic line edge roughness values σ_Δ in this modified likelihood function. As it can be clearly seen, the reconstructed sidewall angles SWA are much closer to the reference value of 90° indicated by the green line, reducing the systematic measurement error introduced by line edge roughness by about one order of magnitude from 2.5° to about 0.25°.

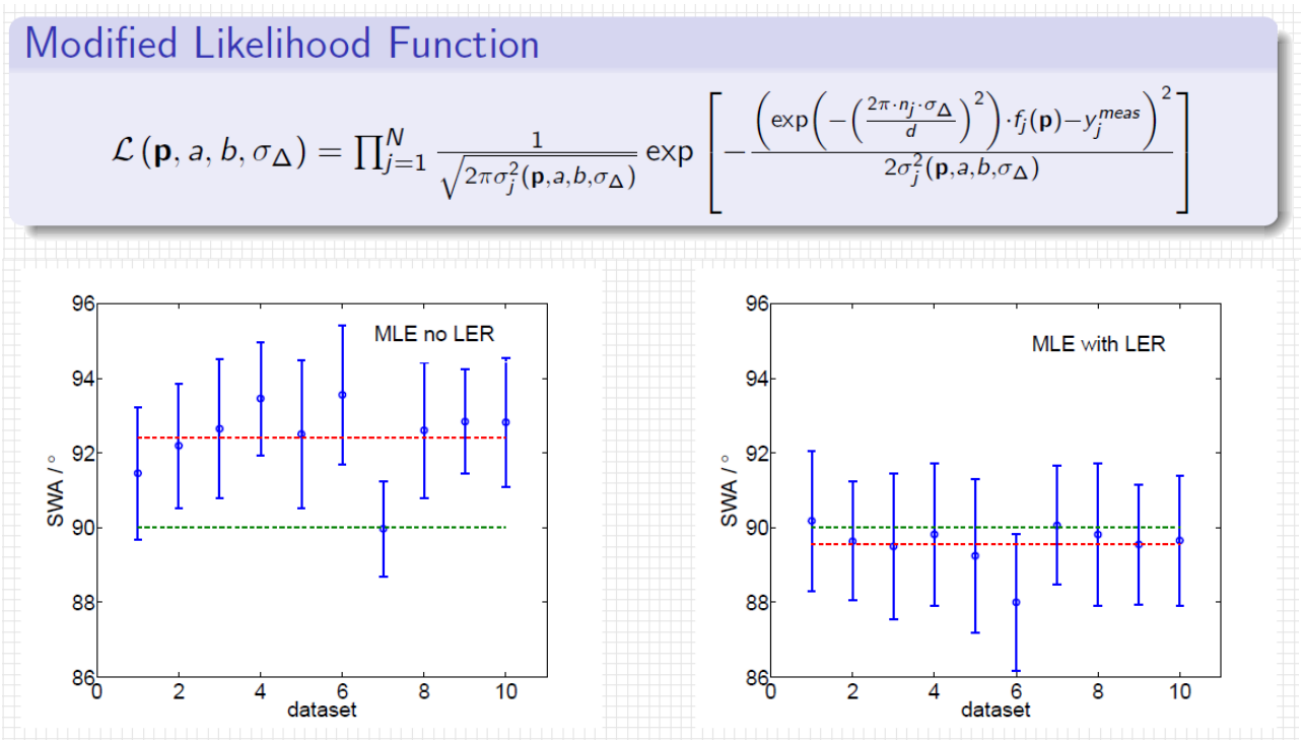

Figure 20. Reconstruction results of the parameter side wall angle for different datasets using the maximum likelihood approach without (left) and with (right) inclusion of realistic line edge roughness values in the modified likelihood function.

For arbitrary (i. e. non-Gaussian) probability distributions of the measurands a more sophisticated approach is required. We developed a Bayesian approach for combined measurement data analysis. Within the Bayesian approach, measurements can be combined and uncertainties are consistently given by the credible intervals of the posterior distribution. This method works well and usually leads to the expected improvements in terms of reduced measurement uncertainties.

Table 2: Reconstruction results of goniometric scatterometry and spectroscopic ellipsometry measurement data obtained for a 1D Si grating, and of a full combined data analysis using the Bayesian approach (comb.).

Sample (nom. p, CD, h)	HZB_P100_CD35(100, 35, 100 nm)		
	Scatt.	M.P.	comb.
CD [nm]	32.3 (1.8)	33.0 (1.5)	32.5 (1.1)
h [nm]	105.7 (2.3)	105.8 (2.2)	105.7 (1.6)
swa [°]	91.4 (1.9)	90.9 (1.6)	91.2 (1.2)
h_oxide [nm]	3.0 (0.6)	3.2 (0.7)	3.1 (0.4)
CR_{top} [nm]	14.9 (3.0)	13.8 (1.9)	14.0 (1.1)
CR_{bottom} [nm]	29.3 (2.8)	30.4 (1.4)	30.1 (1.2)

Table 2 shows a typical reconstruction result for a silicon 1D line grating for two different individual measurement methods, goniometric scatterometry and Mueller polarimetry compared with the result of the combined data analysis of these two data sets applying the Bayesian approach. However, since this approach

requires a time consuming Markov-Chain-Monte Carlo sampling of the posterior distribution, it requires substantial computational resources. Thus, in the near future (outside of this project) we will work on even much faster computational methods based on surrogate models, to improve the handling and applicability of the Baysian approach for combined data analysis.

Conclusion

The maximum likelihood approach was successfully tested and implemented to solve the inverse diffraction problem, which is required to analyse scatterometry measurements. The refinement of the geometry model including more realistic structure parameters led to a significant reduction of the variances in the measurement uncertainty for CD. The Bayesian approach for combined measurement data analysis was developed and applied to combine consistently scatterometry and AFM measurements. AFM data was used as *a priori* knowledge. In particular, for this purpose, the software package GSvit-scattering was developed for direct calculation of far field diffraction patterns from AFM data, applicable both for periodic and randomly rough surfaces. It was demonstrated that the combination of both measurement techniques reduced the overall uncertainties which are given as credible interval of the posterior distribution. Sophisticated statistical models for combined data analysis are available now for hybrid metrology approaches combining different scatterometry or even scatterometry and microscopy data, which allows achieving measurement uncertainty levels even lower than obtained for the individual methods alone.

3.5 Design, development, test and calibration of a scatterometry standard

Introduction

The procedure to achieve an in-depth understanding of the measurement process and to derive a complete measurement budget for a measurement task, which is required to perform traceable measurements, is very complex, in particular for scatterometry because it is an indirect metrology. This procedure can typically not be provided by end users in industry. Instead, traceability can be introduced at the industry level by the availability and applications of suitable calibrated reference standard samples for scatterometry. Therefore we have designed, developed, validated and calibrated two different types of such scatterometry standards for metrology applications on Silicon wavers and on patterned photoresist during the lithographic manufacturing process.

Discussion

Although standards exist which are applicable for AFM and SEM, these standards are not suitable for scatterometry, mainly because the overall size of the structured area is too small. Moreover, there has not even been a suitable standard available for applications in high-end scatterometry. Therefore, an essential objective of this project has been the development of scatterometry reference standards for metrology in the semiconductor industry, in particular for wafer processing including lithography. The availability of high quality and well characterised and calibrated scatterometry standards supports the introduction of accurate and traceable dimensional scatterometry in nanomanufacturing, in particular for nanoelectronic devices. This will significantly improve the accuracy and precision of current manifold applications of scatterometry in the lithographical manufacturing process. In addition it will enable new applications of scatterometry also in quality control requiring absolute metrology. Finally we expect a significant improvement of tool matching between microscopic and optical CD metrology methods due to the availability of such a standard.

The development of the reference standard has been an iterative process which included three optimisation steps.

3.5.1 Design aspects

The design of the scatterometry reference standards took into account different boundary conditions and requirements, so they should be applicable to different instruments available at the NMIs and industry, cover state of the art industry requirements and current lithography technologies and be extendable to future technology steps. Additionally, these standards should be suitable for AFM and SEM characterisation and be relatively easy to manufacture with the available high quality manufacturing processes. It was the project's ambition to gather and align the various metrological requirements of the semiconductor industry in order to

design standards that cover important applications. Thus the standard has been developed using one design and two different materials:

1. Silicon gratings on a silicon wafer substrate
2. A dielectric material, Si3N4, because of its high stability and high quality manufacturability

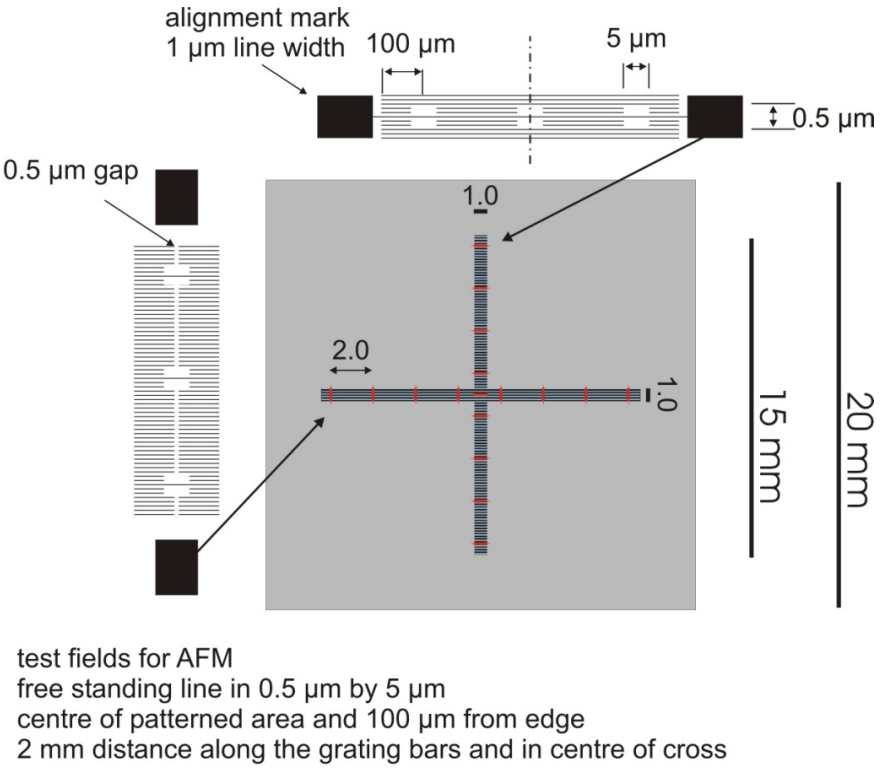

Figure 21. Design of the first test samples to test and validate the manufacturing processes as well as the applicability of different metrology tools. The large cross shaped grating was chosen to enable GISAXS measurements with the plane of incidence along and perpendicular to the grating lines. The red lines mark areas of locally lowered line-to-space ration to enable AFM reference measurements even for small periods below 100 nm.

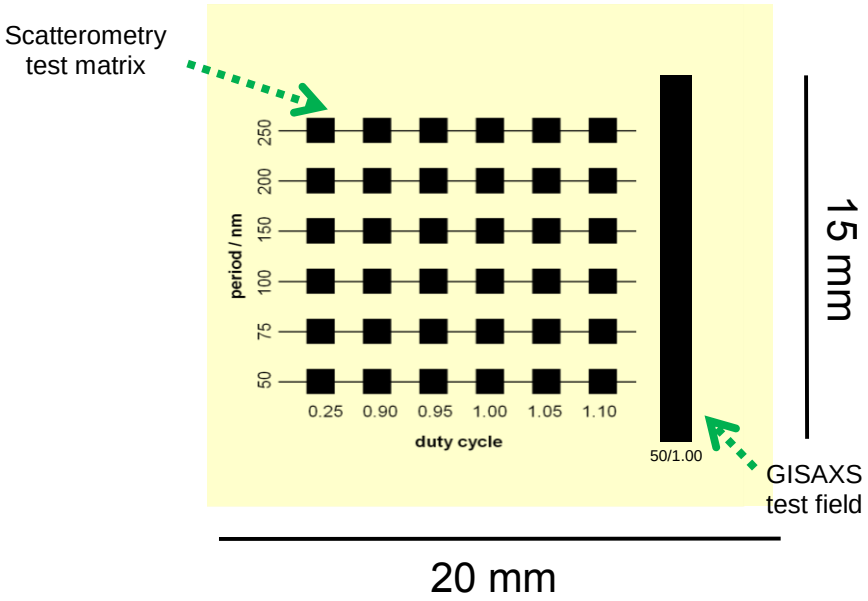

Figure 22. Draft of the final standard design containing only one GISAXS test field (plane of incidence along the grating lines) for GISAXS reference measurements and to test the process quality. Additionally a matrix of smaller 1 mm^2 scatterometry targets is added to enhance the parameter space for scatterometer characterisation. The low line-to-space ratio in the left column enables a more direct comparison with AFM reference measurements even for small periods.

The requirements and specifications of the standards have been thoroughly discussed with the project collaborators and stakeholders, such as ASML, NIST (USA) and SEMATECH.

For the first and intermediate tests the samples have been manufactured with the design shown in figure 21, containing essentially two 15 mm X 1 mm large grating structures, one with the grating structures oriented parallel to the plane of incidence and one with perpendicular oriented structures. This design has been chosen to enable GISAXS measurements and testing. For other scatterometry and SEM measurements, special additional finding structures have been added to identify measurement areas of more local probing methods. Additionally, areas of locally lowered line-to-space ratio have been added to enable AFM reference measurements even for small periods below 100 nm.

For the final standard design we have developed a modified design (Figure 22). This design contains only one GISAXS test field (plane of incidence along the grating lines) for GISAXS reference measurements and to test the process quality. In addition, a matrix of smaller 1 mm^2 scatterometry targets is added to enhance the parameter space for scatterometer characterisation. The low line-to-space ratio in the left column enables a more direct comparison with AFM reference measurements even for small periods.

So far the produced reference standards cover a range of grating periods between 50 nm and 250 nm and nominal CD values between 25 nm and 100 nm. The structure height was adapted for different grating periods to ensure the best manufacturing quality.

3.5.2 Process development and manufacturing

The reference samples and scatterometry standard for this project were manufactured by electron beam lithography (cf. Figure 23). The substrates used were silicon wafers for the silicon gratings and silicon wafers with a deposited 100 nm silicon nitride layer for the dielectric gratings.

HZB has identified and optimised a suitable process for the manufacturing of a Si and the Si_3N_4 version of the reference standards. For CD values > 50 nm, an approximately 90 nm thick resist layer was spin coated onto the wafer. For CD values ≤ 50 nm, thinner resist layers were utilised, with thicknesses down to 30 nm for the smallest CD of 25 nm. After spin coating, a pre-exposure bake was performed to remove the solution from the resist layer. For the electron beam exposure, a Vistec EBPG5000+ES e-beam writer was used, which operates

with an electron acceleration voltage of 100 kV. A proximity correction was also applied. The final step involves reactive ion etching (RIE) of the wafer, while the resist acts as etch mask. The etching gases used for the silicon gratings were SF_6 and C_4F_8, the former being responsible for selective etching of silicon (as opposed to the organic polymer) while the latter acts as passivation layer enabling highly anisotropic etching, which results in lines & spaces with approximately vertical side walls. For etching the dielectric gratings, CHF_3 was used. Finally, the remaining resist layer was removed in the RIE system with oxygen plasma. The electron beam writer addresses typically main field sizes of 250 µm x 250 µm. Further distribution of the design over the whole sample size is done by scanning the sample itself via a laser interferometrically controlled stage. Although the individual fields are periodically aligned by an automatic adjustment of the beam deflection on designated markers on the sample holder table during the exposure, small drifts of the sample or holder system due to slight variations in temperature may lead to minor stitching errors between adjacent fields. Normally, these stitching errors are too small to have an impact on the design or to be measured e.g. by scanning electron microscopy. Interestingly, even the periodicity of sub-fields of 4.3 µm in the e-beam writing process is visible in the GISAXS measurement at the PTB.

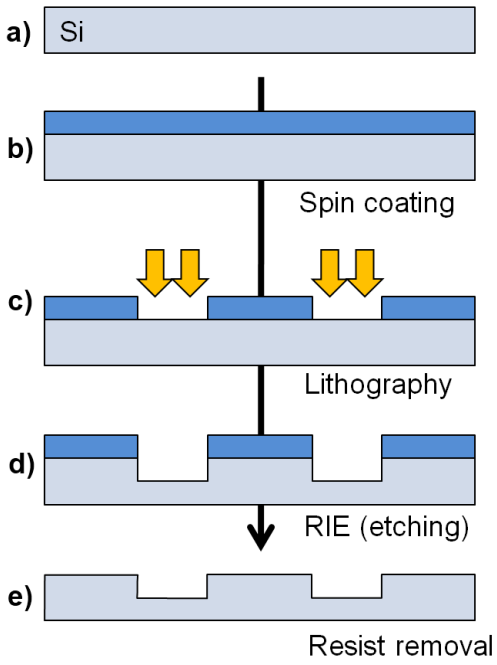

Figure 23. Fabrication Process: A silicon wafer (a) is coated with resist (b), which is subsequently exposed by an electron beam (c), transferring the design to the resist. The exposed resist is removed during development (c). Using reactive ion etching, the resist pattern is transferred to the Si wafer (d). Finally, the resist is removed in oxygen plasma (e).

3.5.3 Sample characterisation

The quality of the fabricated grating samples and detailed features of the line structures have been characterised using high resolution microscopy tools, namely low voltage SEM and 3D AFM. Figure 24 shows a measurement example of AFM line edge and line widths roughness measurements on test samples for the first iteration stage.

Figure 25 shows SEM measurement examples of the final standard structures for both materials (Si and Si_3N_4). Measurements have been done using top down and cross section images, the latter of course only on identically manufactured test samples, because cross section imaging is a destructive method. The top down SEM images shows rather smooth line edges. There are, however, some hints for perturbations with a longer correlation length. Also the cross section SEM revealed some issues in particular for the Si gratings, which

were confirmed by the scattering data. The bottom of the etched grooves is not plane but rather curved with almost constant radius across its full width. The top corners of the lines were much better defined. This was easily understood from the fabrication process, as the grooves were etched after resist development with the top area of the lines covered by the resist acting as the etch mask and thus protected. After etching, the resist was stripped by an oxygen plasma treatment which does not further etch the sample. This treatment, however, oxidized the surface and caused a rather large oxide thickness of around 6 nm. It should be noted that this oxide is not a stoichiometric SiO_2 and probably also not homogeneous from the silicon interface to the surface. For the manufactured Si_3N_4 gratings the bottom corner rounding is less pronounced as compared with the Si gratings.

The microscopic characterisation has been validated by scatterometric measurement in the DUV and X-ray spectral range using EUV-SAS and GISAXS. From the cross section SEM images we have derived the geometry model shown in Figure 26 using a trapezoidal cross line cross section with top and bottom corner rounding as a suitable and sufficiently realistic structure profile description.

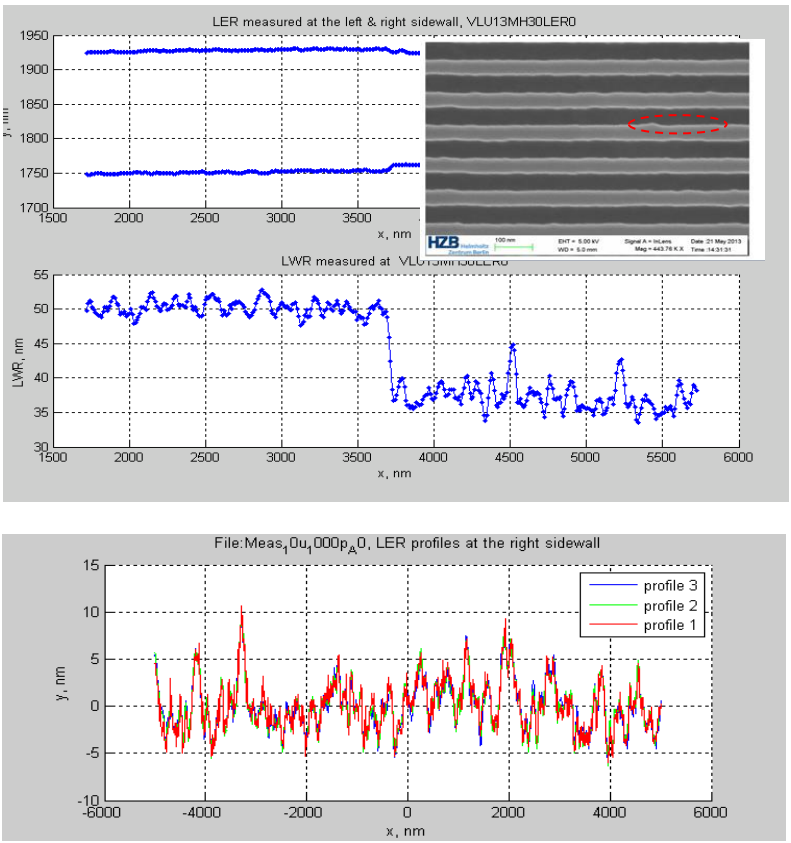

Figure 24. Examples of AFM line edge roughness measurements. Top: a first stage test sample manufactured by HZB shows clearly a significant irregularity in the linewidth and edge position, probably due to not perfect stitching. Bottom: different scans along the edge using the vector approach scanning shows an excellent reproducibility of the results and demonstrate the high sensitivity and reliability of this method.

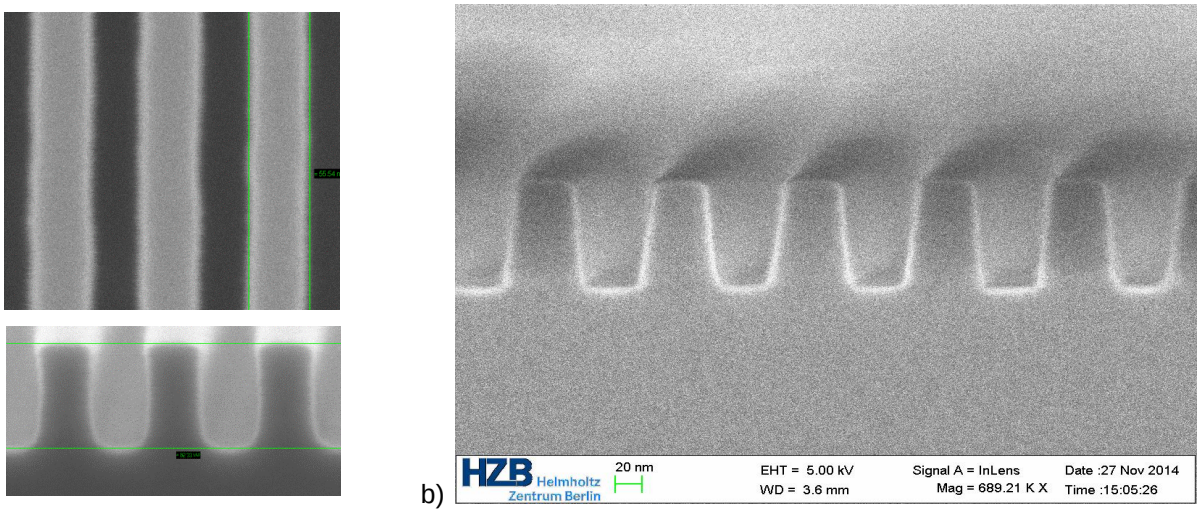

Figure 25. a) SEM top-down and cross section images of a Si sample, showing nearly upright edge profiles but a significant amount of especially bottom corner rounding; b) the SEM cross section image of a Si_3N_4 sample shows much less bottom corner rounding, but less steep edges.

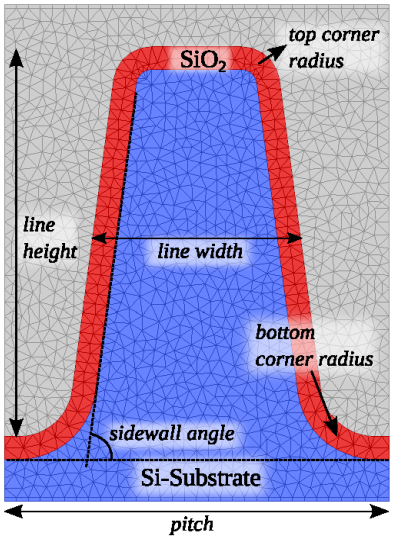

Figure 26. Scheme of the geometrical model used for the data evaluation. The six parameters are indicated.

For the model, we assumed a homogeneous thickness of the oxide, which results from oxygen plasma cleaning for resist stripping, at all surfaces. From the cross section SEM (Figure 25) it was known that the top corners of the lines are rather sharp while there is significant rounding at the bottom edges. This model includes 6 variable parameters, the line width (CD), height, edge angle, top and bottom corner rounding and the thickness of the oxide layer, and has been applied for the evaluation of all scatterometry measurement data obtained at both type of standard samples. The remaining assumptions and corresponding approximations are the symmetry of both edges as well as the homogeneity of the oxide layer at top, bottom and at the line edges.

Figure 27 show examples of scatterograms measured with EUV-SAS and GISAXS and the corresponding best fit results of the profile reconstruction. The reconstruction parameters are found as best fit solution between measurement data and the rigorously calculated data by means of a standard nonlinear optimization scheme, which combines a global optimization strategy based on particle swarm algorithm with a local optimization routine using standard gradient based methods. This combination ensures that the global minimum is found. The calculated intensities for the optimized geometry are also shown in Figure 27.

Figure 28 shows example results for DUV scatterometry measurements on two different samples with grating periods as small as 100 nm (left side) and 50 nm (right). Similarly to the reconstruction procedure described above for the GISAXS and EUV-SAS, data have been analysed. The blue curves show the best fit solutions. The comparison of the reconstructed structure profiles with cross section SEM images of identically manufactured grating samples demonstrate that even structure details such as the bottom and top corner rounding were well reconstructed. Furthermore, the agreement with profiles reconstructed from the X-ray

measurements was also very good. This demonstrates the high reliability and performance reached within this project for the investigated scatterometric methods.

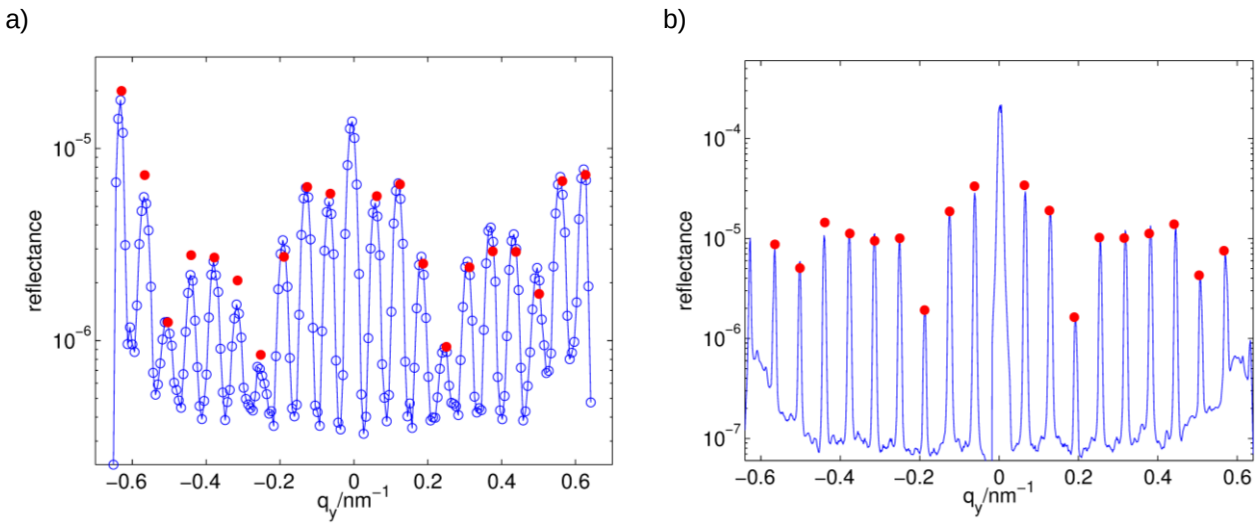

Figure 27. Example scatterograms measured with a) EUV-SAS at photon energy of 1225 eV at an angle of incidence of 84.0° and b) GISAXS at 6.5 keV at 88.9° AOI. The measured data are shown in blue. The red dots indicate the reconstructed intensity values for the best-fit geometry.

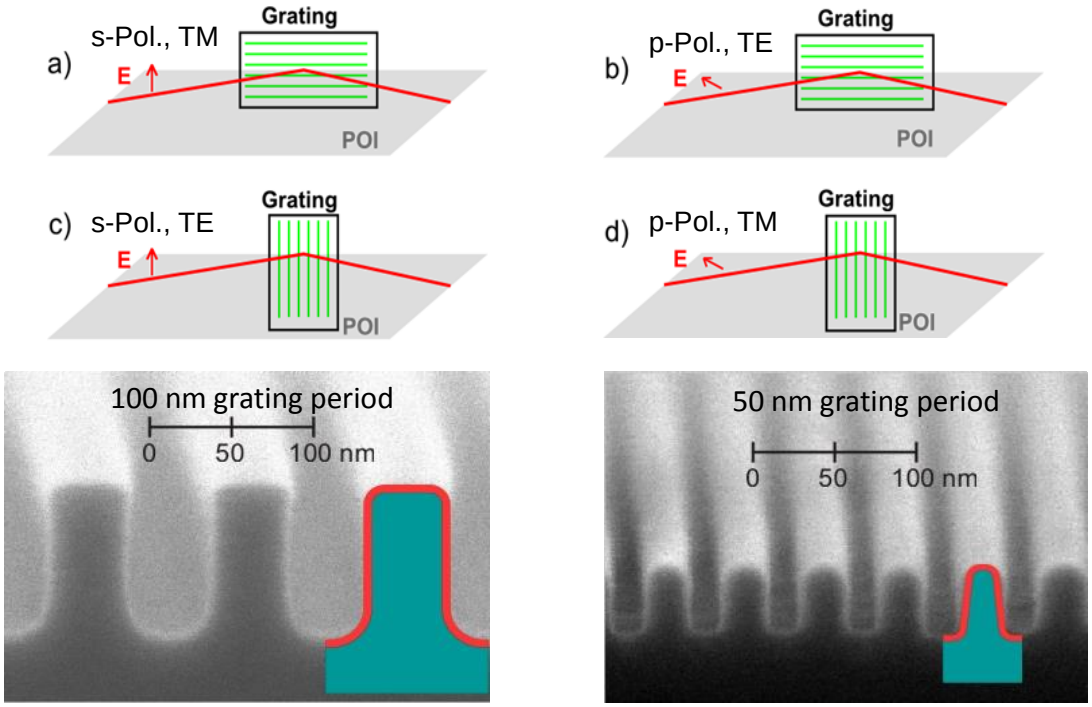

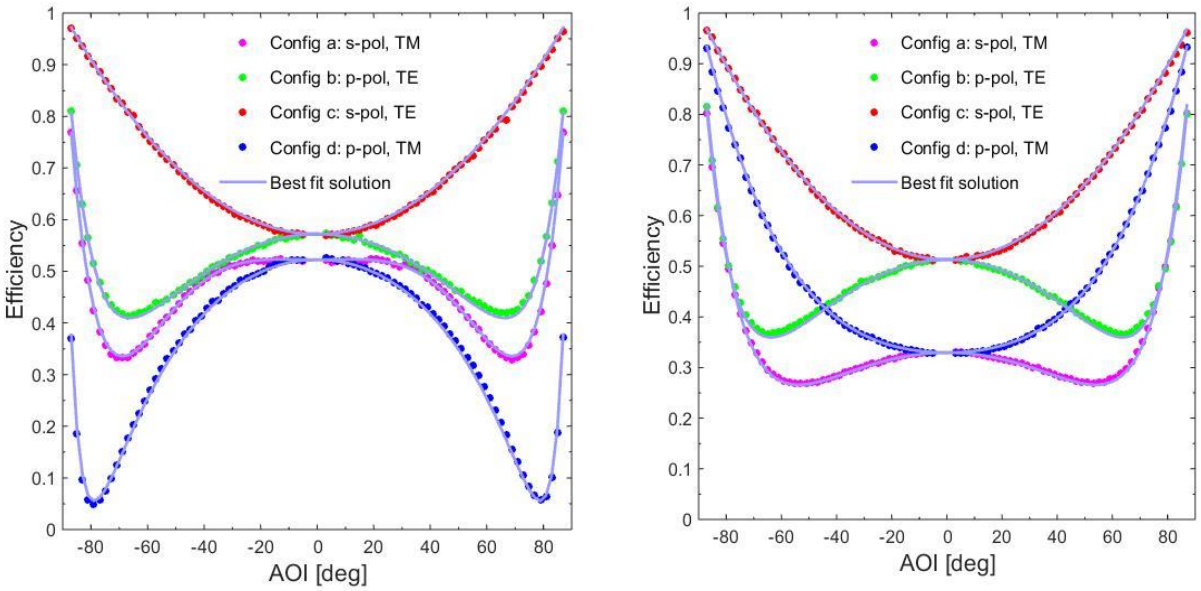

Figure 28. Measurement results obtained with DUV scatterometry: top – previous page) four different measurement configurations are applied for sub-wavelength gratings; middle – previous page) corresponding best fit reconstruction results compared with cross section SEM images; bottom – this page) measured reflectance versus the angle of incidence for gratings with a period of 100 nm (left) and 50 nm (right);.

3.5.4 Calibration

The geometrical parameters measured with GISAXS, EUV-SAS and DUV-Scatterometry are summarised in table 3. Data show different reproducibility for different geometry parameters as reconstructed from different datasets. The parameter with best reproducibility is the structure height. For the CD, we obtained larger deviations which are coupled with significant variations of the side wall angle (SWA) and bottom corner rounding. The steepest SWA, e.g., always correlates with largest bottom corner radius. The variations in the apparent oxide thickness may be due to the inhomogeneous nature of the oxide which was created by the oxygen plasma cleaning for resist stripping. Here, a further refinement of the model may be needed.

Table 3: Measurement results of geometrical reconstruction of grating profiles from GISAXS, EUV-SAS and DUV scatterometry.

Sample	method	CD / nm	line height / nm	SWA /°	SiO_2 thickness / nm	top radius / nm	bottom radius / nm
	GISAXS	25.1	48.2	87.7	'-	4.2	13.8
Si-50-25	EUV-SAS	23.3	48.9	88.6	4.7	6.4	11.6
	DUV-Scatt.	24.8	51.7	84.4	4.5	9.5	5.0
	GISAXS	48.0	100.3	88.8	4.1	6.8	23.1
Si-100-45	EUV-SAS	45.8	100.9	83.1	6.2	7.8	13.4
	DUV-Scatt.	40.5	101.0	90.9	4.6	3.6	28.9
	GISAXS	55.0	102.1	82.9	5.3	5.7	14.0
Si-100-55	EUV-SAS	53.6	100.8	87.6	8.7	2.9	15.8
	DUV-Scatt.	53.4	101.2	90.0	5.3	8.0	20.5

However, all results of these three methods already agree quite well. The largest variation e. g. for the linewidth being less than 2 nm, which indicates that a pure scatterometric calibration of these standard samples at an uncertainty level of a few nm will very likely be feasible. Furthermore, for the final calibration of these samples the measurement data will be supplemented by top level microscopy measurements using PTB's metrological 3D AFM as described above and PTB's Electron Optical Metrology System (EOMS), an interferometer controlled traceable low voltage CD-SEM, and by spectroscopic data using Ellipsometry and Mueller polarimetry. Combining all these measurement data by applying the methods for combined data analysis developed within this project finally the aimed measurement uncertainty of the order of 1 nm for CD calibration of the scatterometry standard will very likely be reached.

PTB as well as other NMIs (VSL, DFM) are going implement a corresponding calibration service for the developed standards to make them available for support of and applications in industry.

Conclusion

With these results, reliable and high quality scatterometry reference standards are available for the first time, which are well characterised and calibrated, enabling a meaningful calibration of scatterometry tools in industry and therefore leading to traceable and accurate measurements in industrial applications. These standards are available as silicon gratings and as silicon nitride gratings, which are as dielectric gratings much closer to applications in resist metrology. Finally they can also be used to improve tool matching between microscopic and scatterometric measurement systems in industry.

4 Actual and potential impact

4.1 Dissemination

The project and the scientific and technical results described above have been extensively presented in 79 presentations at national and international conferences (e.g. SPIE conference Modelling Aspects in Optical Metrology 2013, chaired by the project coordinator, and the Nanoscale 2013) and workshops, with some of those presentations being invited keynotes. Moreover, these results have been published in 19 peer reviewed publications and 23 conference proceedings, and at least 4 more peer reviewed publications are scheduled for the near future. Additionally, training activities have been offered to the stakeholder community in August 2013 in Berlin and in the context of an international EOS summer school in advance of the EOSAM 2014.

To promote the dissemination of the project outcomes, the partners have organised a successful scatterometry workshop as part of the Annual Meeting of the European Optical Society (EOSAM 2014) in Berlin, Germany. The workshop attracted 60 participants and included a special session dedicated to this project. In total the project results have been presented in 10 talks given at this workshop and 3 more papers in another EOSAM subconference.

This project's results have been discussed regularly with stakeholders from the scientific and industrial communities and also via personal contacts with e.g. Carl Zeiss AG, ASML, NIST, SENTECH and the AMTC. NIST, ASML and SEMATECH have been actively involved in discussions regarding the scatterometry reference standards. The coordinator has supported NIST in organising the annual SPIE conference Instrumentation, Metrology, and Standards for Nanomanufacturing on 20th August 2013 in San Diego, USA as a member of the program committee of this conference. Furthermore PTB is member member of the German Arbeitskreis Ellipsometrie (AKE) Paul Drude e. V., where many ellipsometry companies and users were involved and has discussed with some other members the specific requirements of spectroscopic ellipsometers on a scatterometry standard. Several project participants have visited the AKE international workshops on ellipsometry in March 2013 in Leipzig and 2014 in Dresden for dissemination of project results as well as for further detailed exchange with many stakeholders (e. g. SENTECH, Osiris GmbH, NamLab Dresden). The stakeholders have always been invited to join the project meetings and, for example, ASML has joined regularly.

4.2 Impact on standardisation

The progress of this project, in particular the developed scatterometry reference standards and the status of the SEMI Guide to establishing uncertainties of scatterometry measurements have been discussed with members of the SEMI Microlithography committee. Further development of this guide has been stopped by the chairman of the corresponding SEMI Scatterometry Task Force (NIST), but based on the results of this project a future discussion is planned aiming to revert that decision.

4.3 Impact on the metrology and scientific communities

Overall achievements can be summarised as follows:

The traceability and accuracy of scatterometric methods has been significantly improved from an uncertainty above 10 nm, at the beginning of this project, to a few nm for individual methods and to a level of about 1 nm for CD calibration of the scatterometry standard. This has been achieved by:

- Evaluating and quantifying the impact of many approximations and simplifying assumptions on the measurement results. This has enabled much more complete and reliable measurement uncertainty estimations and led to significant reductions in the measurement uncertainties even for conventional scatterometry methods.

- Developing and evaluating novel methods such as Mueller polarimetry, Coherent Scanning Focused Beam Scatterometry and X-ray scatterometry GISAXS and EUV-SAS. In particular, the high metrological potential of x-ray scattering methods have been demonstrated and GISAXS is available now for high sensitivity and accuracy measurements.

- Developing statistical models for combined data analysis, which are available now for hybrid metrology approaches combining different scatterometry or even scatterometry and microscopy data, which allows to achieve measurement uncertainty levels even lower than obtained for the individual methods alone.

- Significantly improving 3D capability of scatterometry by better modelling and scatterometry methods. Much faster algorithms in combination with parameterisation of 3D-problems were implemented in an efficient software module that is now available for analysis of 3D scatterometry data. Three different scatterometry methods for advanced 3D metrology (Fourier scatterometry, sectioning goniometric scatterometry and GISAXS) have been tested and validated for 3D measurements.

- Making available for the first time scatterometry metrology solutions for the optics industry to characterise fast and efficiently diffractive and hybrid (i. e. diffractive-refractive) structures and to support the manufacturing process. Two methods based on goniometric scatterometry and Mueller polarimetry have been successfully tested on different diffractive samples on flat as well as curved substrates and are ready for applications in optics industries.

- Developing and testing unique atomic force microscopes with promising outstanding features such as long range 3D capabilities to enable statistically relevant comparisons with the integral measuring scatterometry methods both on structure detail measurements, such as edge roughness, and on the main structure parameters CD, edge angle and height.

- For the first time, reliable and high quality scatterometry reference standards are available, which are well characterised and calibrated, enabling a meaningful calibration of scatterometry tools in industry and with it traceable and accurate measurements in industrial applications. These standards are available as silicon gratings and as silicon nitride gratings, which are (as dielectric gratings) much closer to applications in resist metrology. Finally they can be used additionally to improve the tool matching between microscopic and scatterometric measurement systems in industry.

Software developed within the project will be used and further developed after the end of this project, either as part of the company services of JCMwave GmbH or as an open source application (CMI). The developed methodology for numerical simulations is part of the software documentation and will be available to other users of the software. These existing software solutions with enhanced capabilities and specific features (e. g. enhanced 3D capabilities, fast algorithms and procedures for combined data analysis to support future developments in hybrid metrology) are already in use by the scientific and metrology community, as well as in industrial applications.

The measurement comparison on the development on scatterometry standards has made it possible for different partners such as DFM and PTB to offer a calibration service for scatterometry standards from 2015.

4.4 Impact on the industrial and other user communities

Direct uptake of the project's outputs, in particular low cost diffractive optics, provides European manufacturers such as Nanocomp access to fast and efficient optical metrology for manufacturing. This will enable improved and faster quality control and process development supporting the success and growth of manufacturers of diffractive optics. In particular, Nanocomp has shown great interest on the VTT scatterometer and is planning to either use a measurement service from VTT or build its own scatterometer based on the knowledge obtained in this project. Both options significantly benefit from the work done in the project.

Different stakeholders such as manufacturers of scatterometry-based metrology tools and European manufacturers of integrated circuits have shown interest in the developed reference standard samples, and it is expected that several stakeholders will use these standard samples as soon as they are commercially available. The availability of reliable scatterometry reference standard samples and the knowledge and methods developed in this project will support manufacturers e. g. ASML, SENTECH in the development of their products and therefore contribute to support their already strong international European position.

Following on from the suggestion and interest of the Advanced Mask and Technology Center (AMTC), PTB has started testing novel EUV photomasks currently developed by the AMTC for their new mask manufacturing processes. This testing takes advantage of EUV scatterometry, AFM, optical scatterometry and GISAXS facilities further developed in this project.

4.5 Long term impact

The improved and partly novel metrology capabilities developed within this project are already contributing to the development of new and better products of European semiconductor companies and in the longer term will contribute to sustain and extend the success of the European and international semiconductor industry.

In particular, the work on Mueller polarimetry and subwavelength scatterometry has a strong potential for applications in research and development. High-end nanoelectronics and (micro-) optics and photonics are key technologies, which in the future, will enable novel or improved products and applications. The mentioned technologies affect a substantial part of new technological developments. New improved and miniaturised electronics enable more efficient electronic devices and improved electronic control elements e.g. for automotive applications. New miniaturised micro-optical components are used for example in newly developed optical sensors for environmental analytics. Within this project we have worked on the development of a reliable and efficient metrology for novel diffractive and hybrid optics as well as for upcoming technology nodes in the semiconductor industry.

5 Website address and contact details

More info and details about the project and results are available at the project website:

http://www.ptb.de/emrp/ind17.html

The contact person for general questions about the project is Dr Bernd Bodermann, PTB: bernd.bodermann@ptb.de +49 531 5924222 Bundesallee 100, D-38116 Braunschweig, Germany

6 List of publications

[1] M.-A. Henn, H. Gross, F. Scholze, M. Wurm, C. Elster, M. Bär: *A maximum likelihood approach to the inverse problem of scatterometry,* Opt. Express **20** (2012), 12771-12786

[2] M. Karamehmedovic, P-E. Hansen, K. Dirscherl, E. Karamehmedovic, T. Wriedt: *Profile estimation for Pt submicron wire on rough Si substrate from experimental data,* Opt. Express **20** (2012), 21678-21686

[3] N. Kumar, O. El Gawhary , S. Roy, S. F. Pereira, H. P. Urbach: *Phase retrieval between overlapping orders in Coherent Fourier Scatterometry using scanning*, JEOS **8** (2013), 13048

[4] S. Heidenreich, H. Gross, M.-A. Henn, C. Elster, M. Bär: *A surrogate model enables a Bayesian approach to the inverse problem of scatterometry*., J. Phys.: Conference Series **490** (2014), 012007-1 - 012007-4

[5] H. Gross, S. Heidenreich, M.-A. Henn, G. Dai, F. Scholze, M. Bär: *Modelling line edge roughness in periodic line-space structures by Fourier optics to improve scatterometry*, JEOS **9** (2014), 14003-1 - 14003-10

[6] A. Kato, S. Burger, F. Scholze: *Analytical modelling and 3D finite element simulations of line edge roughness in scatterometry* Applied Optics **51**, 6457 (2012)

[7] H. Gross, M.-A. Henn, S. Heidenreich, A. Rathsfeld, M. Bär: *Modelling of line roughness and its impact on the diffraction intensities and the reconstructed critical dimensions in scatterometry,* Appl. Opt. **51** (2012), 7384-7394

[8] J. Wernecke, F. Scholze, and M. Krumrey: *Direct structural characterisation of line gratings with grazing incidence small-angle x-ray scattering*, Rev. Sci. Instrum. **83** (2012), 103906

[9] S. Roy, N. Kumar, S. F. Pereira, H. P. Urbach: *Interferometric coherent Fourier scatterometry: a method for obtaining high sensitivity in the optical inverse-grating problem*, J. Opt. **15** (2013), 75707

[10] M. A. Henn, S. Heidenreich, H. Gross, A. Rathsfeld, F. Scholze, M. Bär: *Improved grating reconstruction by determination of line roughness in extreme ultraviolet scatterometry*, Opt. Lett. **37** (2012), 5229-5231

[11] H. Husu, T. Saastamoinen, J. Laukkanen, S. Siitonen, J. Turunen, A. Lassila: *Scatterometer for characterisation of diffractive optical elements*, Meas. Sci. Technol. **25** (2014), 044019

[12] J. Endres, A. Diener, M.-A. Henn, S. Heidenreich, M. Wurm, B. Bodermann: *Investigations of the influence of common approximations in scatterometry for dimensional nanometrology*, Meas. Sci. Technol. **25** (2014), 044004

[13] R. Koops, V. Fokkema: *An approach towards 3D sensitive AFM cantilevers*, Meas. Sci. Technol. **25** (2014), 044001

[14] G. Dai, K. Hahm, F. Scholze, M.-A. Henn, H. Gross, J. Fluegge and H. Bosse: *Measurements of CD and sidewall profile of EUV photomask structures using CD-AFM and tilting-AFM*, Meas. Sci. Technol. **25** (2014), 044002

[15] M.-A. Henn, H. Gross, S. Heidenreich, F. Scholze, C. Elster and M. Bär: *Improved reconstruction of critical dimensions in extreme ultraviolet scatterometry by modelling systematic errors,* Meas. Sci. Technol. **25** (2014), 044003

[16] J. Wernecke, C. Gollwitzer, P. Müller, M. Krumrey: *Characterisation of an in-vacuum PILATUS 1M detector,* J. Synch. Rad. **21** (2014), 529 - 536

[17] Gross, H.; Heidenreich, S.; Henn, M.-A.; Bär, M.; Rathsfeld, A: *Modelling aspects to improve the solution of the inverse problem in scatterometry*, Discrete and Continuous Dynamical Systems - Series S (DCDS-S) **8** (2015), 497 - 519

[18] N. Kumar, P. Petrik, G. K. P. Ramanandan, O. El Gawhary, S. Roy, S. F. Pereira, W. M. J. Coene, H. P. Urbach: *Reconstruction of sub-wavelength features and nano-positioning of gratings using coherent Fourier scatterometry*, Opt. Expr. **22** (2014) 24678.

[19] P. Petrik, N. Kumar, M. Fried, B. Fodor, G. Juhasz, S. F. Pereira, S. Burger, H. P. Urbach *Fourier ellipsometry – an ellipsometric approach to Fourier scatterometry,* J. Eur. Opt. Soc.-Rapid **10** (2015), 15002

Conference proceedings

[20] B. Bodermann, E. Buhr, H.-U. Danzebrink, M. Bär, F. Scholze, M. Krumrey, M. Wurm, V. Korpelainen, P.-E. Hansen, P. Klapetek, M. v. Veghel, A. Yacoot, S. Siitonen, O. El Gawhary, S. Burger, T. Saastamoinen: *Joint Research on Scatterometry and AFM Wafer Metrology*, AIP Conf. Proc. **1395** (2011), 319

[21] B. Bodermann, S. Bonifer, E. Buhr, A. Diener, M. Wurm *High precision dimensional metrology of periodic nanostructures using laser scatterometry* Proc. of the IMEKO TC14 LMPMI Symposium (2011):

Symposium on Laser Metrology for Precision Measurement and Inspection in Industry, Braunschweig, GERMANY
[22] B. Bodermann, J. Endres, H. Groß, M.-A. Henn, A. Kato, F. Scholze, M. Wurm *Towards traceability in scatterometric-optical dimensional metrology for optical lithography,* Proc. of the 113. annual meeting of the DGaO (2012), A028-6B
[23] B. Bodermann, P.-E. Hansen, S. Burger, M.-A. Henn, H. Groß, M. Bär, A. Kato, F. Scholze, J. Endres, M. Wurm: *First steps towards a scatterometry reference standard*, Proc SPIE **8466** (2012), 84660E
[24] H. Gross, M. A. Henn, S. Heidenreich, A. Rathsfeld, M. Bär: *Impact of line edge and line width roughness on diffraction intensities in scatterometry,* Proc SPIE **8550**, 85503R (2012)
[25] S. Burger, L. Zschiedrich, J. Pomplun, F. Schmidt, B. Bodermann: *Fast simulation method for parameter reconstruction in optical metrology* Proc. SPIE **8681** (2013) , 868119
[26] V. Soltwisch, S. Burger, F. Scholze: *Scatterometry sensitivity analysis for conical diffraction versus in-plane diffraction geometry with respect to the side wall angle,* Proc. SPIE **8789** (2013), 878905
[27] J. Endres, S. Burger, M. Wurm, B. Bodermann: *Numerical investigations of the influence of different commonly applied approximations in scatterometry,* Proc. SPIE **8789** (2013) , 878904
[28] M. A. Henn, S. Heidenreich, H. Gross, B. Bodermann, M. Bär: *The effect of line roughness in DUV scatterometry*, Proc. SPIE **8789** (2013) , 87890U
[29] S. Heidenreich, M. A. Henn, H. Gross, B. Bodermann, M. Bär: *Alternative methods for uncertainty evaluation in EUV scatterometry*, Proc. SPIE **8789** (2013) , 87890T
[30] P.-E. Hansen, S. Burger: *Investigation of microstructured fibre geometries by scatterometry,* Proc. SPIE **8789** (2013), 87890R
[31] S. Burger, L. Zschiedrich, J. Pomplun, F. Schmidt: *Finite-element based EMF simulation methods for computational lithography and computational metrology in the DUV and EUV regimes*, Proc. SPIE **8880** (2013), 88801Z
[32] J. Endres, B. Bodermann, G. Dai, H. Gross, M. Wurm, M.-A. Henn, F. Scholze: *Comparison of DUV scatterometry for CD and edge profile metrology on EUV masks,* Fringe 2013: 7th International Workshop on Advanced Optical Imaging and Metrology (2014), 695 - 700, Springer 2013
[33] F. Scholze, V. Soltwisch, G. Dai, M.-A. Henn, H. Gross: *Comparison of CD measurements of an EUV photomask by EUV scatterometry and CD-AFM,* Proc. SPIE **8880** (2013), 88800O
[34] P. Petrik, N. Kumar, E. Agocs, B. Fodor, S. F. Pereira, T. Lohner, M. Fried, H. P. Urbach: *Optical characterisation of laterally and vertically structured oxides and semiconductors*, Proc. SPIE **8987** (2014), 89870E
[35] H. Gross, S. Heidenreich, M. Bär: *Fourier optics for investigating the impact of roughness to scatterometry,* Proc. of the 2014 International Conference on Circuits, Systems, Signal Processing, Communications and Computers (CSSCC '14): Recent Advances in Electrical and Computer Engineering: (2014), OLA-02.pdf, 29 - 34
[36] V. Soltwisch, J. Wernecke, A. Haase, J. Probst, M. Schoengen, M. Krumrey, F. Scholze: *Nanometrology on gratings with GISAXS: FEM reconstruction and Fourier analysis,* Proc. SPIE **9050** (2014), 905012
[37] J. Endres, N. Kumar, P. Petrik, M.-A. Henn, B. Bodermann: *Measurement comparison of goniometric scatterometry and coherent Fourier scatterometry*, Proc. SPIE **9132** (2014), 913208
[38] B. Bodermann, B. Loechel, F. Scholze, G. Dai, J. Endres, J. Probst, M. Schoengen, M. Krumrey, P.-E. Hansen, V. Soltwisch: *Development of a scatterometry reference standard,* Proc. SPIE **9132** (2014), 91320A
[39] Scholze, F.; Bodermann, B.; Burger, S.; Endres, J.; Haase, A.; Krumrey, M.; Laubis, C.; Soltwisch, V.; Ullrich, A.; Wernecke, J: *Determination of line profiles on photomasks using DUV, EUV and X-ray scattering,* Proc. SPIE **9231** (2014), 92310M-1 - 92310M-11
[40] T. Saastamoinen, H. Husu, J. Laukkanen, S. Siitonen, J. Turunen, A. Lassila: *Scatterometric characterisation of diffractive optical elements*, Proc. SPIE **9173** (2014), 917301
[41] Sven Burger, Lin Zschiedrich, Jan Pomplun, Sven Herrmann, Frank Schmidt: *Hp-finite element method for simulating light scattering from complex 3D structures* Proc. SPIE **9424** (2015) 94240Z
[42] Sven Burger, Lin Zschiedrich, Jan Pomplun, Mark Blome, Frank Schmidt: *Advanced finite-element methods for design and analysis of nanooptical structures: Applications* Proc SPIE **8642** (2013) 864205